Check for updates

The effects of variable riverine inputs and seasonal shifts in phytoplankton communities on nitrate cycling in a coastal lagoon

Mindaugas Zilius[1]*, Rūta Barisevičiūtė[2], Stefano Bonaglia[1,3], Isabell Klawonn[4], Elise Lorre[1], Tobia Politi[1,3], Irma Vybernaite-Lubiene[1], Maren Voss[4], Donata Overlinge[1] and Paul A. Bukaveckas[5]

[1]Marine Research Institute, Klaipeda University, Klaipeda, Lithuania, [2]State Research Institute, Center for Physical Sciences and Technology, Vilnius, Lithuania, [3]Department of Marine Sciences, University of Gothenburg, Gothenburg, Sweden, [4]Department of Biological Oceanography, Leibniz Institute for Baltic Sea Research, Rostock, Germany, [5]Center for Environmental Studies, Virginia Commonwealth University, Richmond, VA, United States

Estuarine systems, being situated at the interface between land and marine environments, are important sites for nitrate (NO_3^-) retention and processing due to large inputs, long retention time, and high biogeochemical activity. However, it remains uncertain how pelagic and benthic processes control NO_3^- cycling and how the relative importance of these processes is affected by seasonal changes in estuarine conditions. We measured the suite of processes governing NO_3^- cycling in the Curonian Lagoon (Southeast Baltic Sea) during two time periods representing spring and summer conditions. We show that in spring, benthic dissimilatory and assimilatory NO_3^- processes prevailed, while in summer, pelagic assimilatory processes dominated. During spring, warming temperatures and riverine nitrogen (N) inputs were associated with the onset of diatom blooms. N assimilation by diatoms resulted in the delivery of particulate organic N and organic matter to the benthos, resulting in greater denitrification in the sediments and a flux of NO_3^- from the water column to the sediments. In summer, phytoplankton blooms of buoyant cyanobacteria and high rates of assimilatory uptake dominated, resulting in greater particulate organic N export from the lagoon into the sea. Given the low dissolved inorganic N concentrations in summer, high uptake indicates that the pelagic community possessed a nutritional strategy to efficiently utilize multiple N forms at high rates. Overall, our findings show that diatom-dominated communities foster strong benthic-pelagic coupling, whereas cyanobacteria dominance is associated with pelagic-based N cycling. While this study sheds new light on mechanisms of NO_3^- retention in the Curonian Lagoon, further spatiotemporal resolution is recommended to better represent the variability in rates and to include other Baltic lagoons for a comprehensive understanding of N cycling in shallow estuarine systems.

1 Introduction

Nitrate (NO_3^-) typically dominates the riverine nitrogen (N) load from land to coastal systems worldwide (Peierls et al., 1991; Vybernaite-Lubiene et al., 2018). Agriculture is a major source of NO_3^- resulting in high concentrations in rivers and groundwater, where catchments are dominated by row crop farming (Arheimer et al., 2012; Santos et al., 2021). While implementation of strategies to mitigate N loss from farmland has progressed in recent decades, NO_3^- loads in regions such as the Baltic Sea continue to increase (e.g. Vybernaite-Lubiene et al., 2018). Estuarine systems, being situated at the interface between land and coastal waters, are important sites for NO_3^- retention due to large inputs, long retention time, and high biogeochemical transformation rates (Voss et al., 2011; Asmala et al., 2017; Bukaveckas et al., 2018).

The attenuation of N through-puts in lagoons and estuaries is referred to as the "filter" function. This important ecosystem service is conventionally linked to N-removal processes occurring in sediments (Voss et al., 2010; Anderson et al., 2014; Carstensen et al., 2020; Magri et al., 2020). Here, denitrification and dissimilatory nitrate reduction to ammonium (DNRA) are the main microbial processes that remove NO_3^- since anammox is typically low in estuarine systems (Thamdrup, 2012). DNRA, in contrast to denitrification, transforms NO_3^- to NH_4^+, and the recycled N can thus remain within the system (Giblin et al., 2010; Magri et al., 2020). In the water column, phytoplankton and bacteria uptake is an important mechanism for converting NO_3^- to particulate and dissolved organic N forms (PON and DON; Middelburg and Nieuwenhuize, 2000a; Olofsson et al., 2019). After incorporation into biomass, particulate N may settle where it is remineralized or buried in sediments (Brion et al., 2008).

Various factors can impact NO_3^- assimilation and conversion. Elevated levels of NO_3^- in the water column typically lead to increased uptake rates by phytoplankton and bacteria, which in turn leads to an increase in particulate organic nitrogen (PON) (Middelburg and Nieuwenhuize, 2000b; Twomey et al., 2005; Glibert et al., 2016). Seasonal changes in phytoplankton community composition may influence the quantity and forms of N assimilated (Dortch, 1990; Middelburg and Nieuwenhuize, 2000a; Berg et al., 2003; Lomas and Glibert, 2003). Elevated levels of NO_3^- also stimulate rates of denitrification or DNRA in sediments (Dong et al., 2000, 2009; Magri et al., 2020). The relative importance of these two dissimilatory processes is influenced by the amount of organic carbon in the sediment, the presence of reduced compounds (e.g. H_2S, Fe^{2+}) and the availability of NO_3^- (Kessler et al., 2018; Murphy et al., 2020). Where sediments are exposed to light, NO_3^- respiring bacteria compete for NO_3^- with phytoplankton or microphytobenthos, which can alter the magnitude and direction of sediment-water NO_3^- fluxes (Sundbäck et al., 2006; Risgaard-Petersen, 2003; Bartoli et al., 2021).

The rate of NO_3^- utilization is contingent upon its presence in the water column, which is subject to regulation by riverine inputs, particularly in temperate and boreal estuaries with large seasonal variations in river flow (Bukaveckas et al., 2018; Zilius et al., 2018).

This, in turn, can affect the pathways of NO_3^- transformation and retention (Veuger et al., 2004; Killberg-Thoreson et al., 2021). The different mechanisms involved in the cycling of NO_3^- may respond to seasonal variations in riverine N inputs and the abundance and composition of plankton communities. Attenuation of NO_3^- in estuarine systems is typically attributed to phytoplankton or microbial transformation. Following the conversion of dissolved inorganic nitrogen (DIN) to particulate organic nitrogen (PON), there are two potential pathways for assimilated N: (1) enhanced export of PON (resulting in minimal net N retention), or (2) sedimentation of PON (resulting in net N retention via storage or denitrification). Our prior work documenting input-output fluxes of the Curonian Lagoon (SE Baltic Sea), showed that NO_3^- concentrations in outflowing water were significantly lower relative to riverine inputs (Vybernaite-Lubiene et al., 2017). We found that PON sedimentation was the dominant fate of assimilated N in the spring, whereas remineralization and export of PON were the dominant pathways in summer (Zilius et al., 2018). We hypothesized that seasonal differences in N pathways were dependent on the composition of the phytoplankton community, which can lead to deposition in sediments (in the presence of fast-sinking diatoms) or PON export and remineralization (in the presence of buoyant cyanobacteria). The aim of our work was to quantify these pathways during diatom *vs.* cyanobacteria-dominated conditions.

Concurrent measurements of the diverse processes that regulate NO_3^- concentrations carried out during contrasting environmental conditions could improve our understanding of their role in regulating the supply and demand for N. Although NO_3^- cycling is of considerable importance to understanding eutrophication and recovery, few studies have quantified the multiple processes responsible for NO_3^- turnover (i.e. denitrification, DNRA, and NO_3^- production) in coastal systems (e.g. Bartl et al., 2019; Broman et al., 2021). Simultaneous measurements of pelagic assimilatory processes and benthic dissimilatory processes have not been carried out. In the present study, we measured assimilatory and dissimilatory NO_3^- processes in both the sediment and water column of a large oligohaline lagoon (Curonian Lagoon, SE Baltic Sea). The objectives were (1) to describe the dynamics of NO_3^- cycling in the context of variable riverine inputs and changes in phytoplankton community composition, and (2) to assess the importance of NO_3^- cycling in the context of N throughputs to the sea. For this study, we focused on the cycling of N because it is commonly a limiting nutrient in coastal waters such as the Baltic Sea, and because our prior work has shown that coastal lagoons are important sites for N transformation and retention (e.g. Vybernaite-Lubiene et al., 2017, 2022; Zilius et al., 2018). The findings will complement our prior mass balance studies of the lagoon by providing a mechanistic understanding of specific biogeochemical pathways that comprise the "coastal filter function". By measuring the complex biogeochemical interactions that shape nutrient dynamics in the lagoon systems, we can develop a more robust understanding to inform management and policy decisions aimed at maintaining ecological health.

2 Material and methods

2.1 Study site

The Curonian Lagoon is a large (1584 km^2), shallow (mean depth 3.8 m) waterbody located along the southeast coast of the Baltic Sea (Figure 1). The lagoon is mainly freshwater (mean salinity = 0.2 PSU) due to large riverine inputs and limited exchange with the Baltic Sea through a narrow channel (Zemlys et al., 2013). The lagoon is vertically well-mixed owing to the shallow depth and weak salinity gradients (Zilius et al., 2014, 2020). The Nemunas River is the principal tributary (Vybernaite-Lubiene et al., 2018), accounting for 96% of total water inputs and the main source of nutrients (Jakimavičius and Kriaučiūnienė, 2013; Vybernaite-Lubiene et al., 2022). The lagoon, like the Baltic Sea, is micro-tidal, with lagoon-sea exchanges occurring during periodic wind-forcing events (Zemlys

et al., 2013). On average, riverine inputs (46.2 × 10^6 m^3 d^{-1}) are ~10% lower than the lagoon outflow (50.6× 10^6 m^3 d^{-1}) due to inputs from the Baltic Sea to the lagoon (Vybernaite-Lubiene et al., 2022).

The present study was carried out at two sites (Figure 1) that are representative of the main macroareas of the lagoon (northern and central-southern; Politi et al., 2022), which differ in (1) the influence of riverine inputs, (2) water residence time and (3) sediment characteristics (Zilius et al., 2014, 2018; Umgiesser et al., 2016; Politi et al., 2022). The northern area is characterized by shallower depths (1.5–2 m), proximal riverine inputs, shorter water residence time (seasonal range = 50–100 days), and sandy sediments with low organic matter content (C$_{org}$ < 0.5%) (Umgiesser et al., 2016; Zilius et al., 2018; Politi et al., 2022). The central-southern area of the lagoon is deeper (mean = 2.5 – 5 m) and less affected by riverine inflow. Therefore, this area has a longer water residence time

FIGURE 1
Satellite image by OLI/Landsat-8 (18/09/2014) showing summer blooms in the Curonian Lagoon with stars representing the northern and south-central monitoring stations. Also shown is the location of the monitoring site at the Nemunas River (dark circle). The black line indicates a state border between two countries. The outflow is at the northern end of the lagoon near Klaipeda (panel in the top right).

(seasonal range = 100–250 days) and organic-rich deposits (predominantly silty sediments, C_{org} = 10–14%). Our long-term research has documented differences in pelagic and benthic processes at these two sites (Zilius et al., 2012, 2014, 2018, 2020, 2021a; Bartoli et al., 2021; Broman et al., 2021; Vybernaite-Lubiene et al., 2022; Magri et al., 2024). The two sites exhibit similar patterns of phytoplankton seasonal succession (from diatoms in the spring to cyanobacteria in the summer), but with typically higher maximum abundance at the central-southern site, due to longer water residence time.

We measured a suite of water and sediment processes (Table 1) that would allow us to characterize N cycling on two dates (17 May and 24 August 2021) selected to represent periods when the lagoon is typically dominated by diatoms and cyanobacteria, respectively, and when the availability of nutrients differs. These dates were selected based on routine monthly (April–June, September–November) and summer biweekly (July–August) monitoring of chlorophyll-a and phytoplankton community composition at the two monitoring stations. Given the shallow depths and well-mixed conditions, we obtained vertically integrated water samples (n=3 per site) using a Niskin bottle. Water was transferred to (1) opaque HDPE bottles (2 L) for dissolved nutrient and particulate matter analyses and (2) 20 L jars for assimilation measurements. In addition, five replicate intact sediment cores (i.d. 8 cm, height 30 cm) were collected within 50–150 m of each sampling station using a hand corer for measurement of dissimilatory NO_3^- processes. Bottom water (150 L) was also collected for core maintenance during transportation and incubation activities. During each sampling campaign, vertical profiles of water temperature, salinity, dissolved oxygen, and photosynthetically

active radiation (PAR) were measured *in situ* with a YSI ProQuatro multiple probe (YSI Inc.) and an LI-192 underwater quantum sensor (LI-COR Biosciences). We also monitored dissolved inorganic nitrogen (DIN) concentrations in the Nemunas River (Figure 1) to estimate riverine inputs. River water samples were collected in triplicate at 2-week intervals from January to December 2021, and monthly during the low flow period (May–September). Additionally, on April 30th, a sediment trap (i.d. 14 cm) was deployed at the central-southern site (4 m depth) for three weeks to estimate the gross sedimentation rates (inclusive of suspended and re-suspended particulate matter). The collected material was analyzed to determine dry weight (at 60°C for 48 h) and used to estimate sedimentation rates.

2.2 Measurement of pelagic processes

We used stable isotopes of carbon (C) and N to measure net C-fixation and NO_3^- uptake rates based on a method previously described by Montoya et al. (1996), and Dugdale and Wilkerson (1986). Briefly, 20 250 mL polycarbonate bottles were filled headspace-free with *in situ* water collected integrative from each site, sealed, and assigned to light and dark incubations (see a schematic representation in Appendix, Supplementary Figure S1). A $H^{13}CO_3^-$ ($NaH^{13}CO_3$, 98 atom % ^{13}C, Sigma Aldrich) tracer was injected to a final concentration of 0.2 mM. A $^{15}NO_3^-$ tracer ($Na^{15}NO_3$, 98 atom % ^{15}N, Sigma Aldrich) was injected to a final concentration of 50 μM (May) and 0.5 μM (August), based on ambient concentrations. Incubations lasting from 1.5 to 4 h were conducted with samples collected in triplicates at three time points

TABLE 1 Summary of measured processes and targeted nitrogen (N) transformations during spring and summer periods in the Curonian Lagoon.

Process	Targeted pathway	Type of assessment	Method
Water column			
Net NO_3^- uptake	$NO_3^- \rightarrow PON$	Measured	Incubation with $^{15}NO_3^-$
C fixation	$DIC \rightarrow POC$	Measured	Incubation with $^{13}HCO_3^-$
Autotrophic N demand	DIN, DON $\rightarrow PON$	Calculated	C fixation (light) × N:C
Sedimentation	PON deposition	Measured	Sediment trap
Sediment			
Sediment-water flux	NO_3^- exchange	Measured	Core Incubation
Total denitrification (D_{tot})	$NO_3^- \rightarrow N_2$	Measured	Core incubation with $^{15}NO_3^-$
Denitrification of water column NO_3^- (D_w)	$NO_3^- \rightarrow N_2$	Measured	Core incubation with $^{15}NO_3^-$
Coupled nitrification-denitrification (D_n)	$NH_4^+ \rightarrow NO_3^- \rightarrow N_2$	Calculated	$D_{tot} - D_w$
Total DNRA ($DNRA_{tot}$)	$NO_3^- \rightarrow NH_4^+$	Measured	Core incubation with $^{15}NO_3^-$
DNRA of water column NO_3^- ($DNRA_w$)	$NO_3^- \rightarrow NH_4^+$	Measured	Core incubation with $^{15}NO_3^-$
Coupled nitrification-DNRA ($DNRA_n$)	$NH_4^+ \rightarrow NO_3^- \rightarrow NH_4^+$	Calculated	$DNRA_{tot} - DNRA_w$
River DIN load	Flux to lagoon	Calculated	DIN conc. × river flow

C – carbon, DIC – dissolved inorganic carbon, NO_3^- – nitrate, NH_4^+ – ammonium, DIN – dissolved inorganic nitrogen, DON – dissolved organic nitrogen, PON – particulate organic nitrogen, DNRA – dissimilatory nitrate reduction to ammonium, D_{tot} and $DNRA_{tot}$ represent the sum of processes due to water column NO_3^- (D_w or $DNRA_w$) and coupling with nitrification (D_n or $DNRA_n$).

T_0, T_1, and T_2. A control bottle (no tracers added) was included for each time point. Water samples were incubated in an outdoor tank filled with water to maintain the temperature at 15.0°C and 21.0°C in May and August, respectively. Irradiance at the incubation depth (~25 cm) was 480 (May) and 880 (August) µmol s^{-1} m^{-2}. Samples representing aphotic conditions were covered with aluminum foil. At each time point, a 70–100 mL sample was filtered on a pre-combusted 25 mm Advantec GF75 glass fiber filter (nominal pore size 0.3 µm) for $PO^{13}C$ and $PO^{15}N$ analyses. Additional aliquots were collected and (1) transferred without headspace into 12 ml exetainer (Labco) with 100 µl of 7 M $ZnCl_2$ for ^{13}C in dissolved inorganic carbon (DIC) and (2) filtered and transferred into PE test tubes for nitrate ($^{14}NO_3^-$ + $^{15}NO_3^-$) analysis. All samples were frozen at –20°C until analysis (except for $DI^{13}C$ stored at 4°C).

Net NO_3^- uptake and C-fixation were calculated following Dugdale and Wilkerson (1986) and Montoya et al. (1996), respectively. Net C-fixation in light bottles was used to estimate the total photosynthetic N demand (inclusive of all forms of N) in the euphotic zone based on the C:N ratio of seston (measured at the initial time point). By concurrently using these two tracers, we were able to estimate both the total autotrophic N demand (from C-fixation) and the combined autotrophic and heterotrophic NO_3^- demand. To derive daily values, hourly NO_3^- uptake and C fixation rates in light were used to estimate daytime rates within the euphotic layer taking into account the proportional light dosages during the incubation relative to daily *in situ* values (Bukaveckas et al., 2011). The hourly uptake rates in the dark were used to estimate night-time values and rates in the aphotic layer. The total uptake rates across the water column were calculated from the sum of the depth-integrated uptake in both the aphotic and photic layers.

2.3 Measurements of benthic nitrates flux and dissimilatory reduction processes

In the laboratory, open sediment cores were placed into an incubation tank containing unfiltered, aerated and well-stirred estuarine water in a temperature-controlled room (14.5°C and 21.0°C, respectively in May and August). A stirring bar, driven by an external magnet at 40 rpm, was inserted in each core approximately 15 cm above the sediment interface to maintain water column mixing while avoiding sediment resuspension (Zilius et al., 2018, 2021b). After an overnight preincubation, a gas-tight lid was placed on the top of each core at the start of the dark incubations. For sediment cores collected from the shallower (northern) site in spring, we also conducted incubations under *in situ* light conditions (~60 µmol s^{-1} m^{-2}) to evaluate the impact of light on NO_3^- fluxes. All incubations lasted from 3 to 9 h to keep the final oxygen concentration within 20% of the initial value. To monitor O_2 concentration, two randomly selected cores from each site were equipped with optode sensor spots (FireSting-O2, PyroScience GmbH). At the beginning and end of the incubation, 20 mL water aliquots were collected from each core, and filtered (Frisenette GF/F filters) into 12 mL plastic test tubes for later NO_3^- analysis.

After the flux measurements, cores were opened and left submerged in the incubation tank for ~5 h. Afterwards, NO_3^- reduction was measured following the unrevised isotope-pairing technique (IPT, Nielsen, 1992), which was appropriate here due to relatively low anammox rates in the lagoon sediments (< 4% of total N_2 production; Zilius, 2011). Briefly, all cores were spiked with $^{15}NO_3^-$ tracer (20 mM $Na^{15}NO_3$, 98 atom % ^{15}N, Sigma Aldrich) to a final ^{15}N-label percentage between 51% and 100% depending on background concentrations. The cores were then capped and incubated in the dark as described for fluxes. At the end of incubations, the water and the whole sediment were gently mixed to a slurry. Thereafter, 20 mL aliquots of the slurry were transferred into 12 mL exetainers (Labco) allowing twice overflow, and fixed with 200 µL of 7 M $ZnCl_2$ for later $^{29}N_2$ and $^{30}N_2$ analyses. An additional 40 mL subsample was collected and treated with 2 g of KCl for the determination of the exchangeable NH_4^+ pool and the $^{15}NH_4^+$ fraction. Measured total denitrification (D_{tot}) and DNRA ($DNRA_{tot}$) rates were divided into separate pathways based on the source of NO_3^- (Bonaglia et al., 2014) (Table 1).

Net daily rates were derived by multiplying the hourly rates by the length of the day. When cores were incubated in both light and dark conditions (May, northern site), the net daily rates were calculated by multiplying hourly rates by the mean length of the light and dark periods.

2.4 Analytical methods and phytoplankton analysis

In the laboratory, water samples were filtered within 1–2 h of collection and transferred into 10 ml PE tubes for dissolved inorganic N analysis (DIN) and dissolved silica (DSi). The concentration of DIN (NH_4^+, NO_2^- and NO_{2+3}^-) and DSi was measured with a continuous flow analyzer (San^{++}, Skalar) using standard colorimetric methods (Grasshoff et al., 1983). NO_3^- was calculated by subtracting nitrites (NO_2^-) from the combined nitrite and nitrate concentration (NO_{2+3}^-). Total dissolved nitrogen (TDN) was analyzed by the high temperature (680 °C) combustion, catalytic oxidation/NDIR method using a Shimadzu TOC-V 5000 analyzer with a TNM-1 module. DON was calculated as a difference between TDN and DIN. Water samples for Chl-a were filtered through GF/F filters. Pigments were extracted with 90% acetone (24 h at 4°C) and measured by spectrophotometry (Jeffrey and Humphrey, 1975; Parson et al., 1984). Samples (n=1 per site) for phytoplankton counting were immediately preserved with acetic Lugol's solution and examined at magnifications of 100× and 400× using a LEICA DMI 3000 (Leica Microsystems) inverted microscope. Phytoplankton community composition was determined using the Utermöhl method (Utermöhl, 1958) according to HELCOM recommendations (HELCOM, 2021). Phytoplankton biomass (mg L^{-1}) was calculated according to Olenina et al. (2006) with cell numbers multiplied by species-specific mean cell volumes and assuming a density of 1 g mL^{-1}.

Filters for PON and particulate organic carbon (POC) and their isotopic analyses ($\delta^{15}N$-PON, $\delta^{13}C$-POC) were analyzed with a continuous-flow isotope ratio mass spectrometer (IRMS; Thermo-

Finnigan, Delta S, Thermo Fisher Scientific) at the Leibniz Institute for Baltic Sea Research Warnemünde (IOW). Isotopic samples for $^{29}N_2$ and $^{30}N_2$ production were analyzed by gas chromatography-isotopic ratio mass spectrometry (Thermo Delta V Plus, Thermo Fisher Scientific) with means of a Conflo III interface at the University of Southern Denmark. Samples for $^{15}NH_4^+$ production were analyzed by the same technique after the conversion of NH_4^+ to N_2 by the addition of alkaline hypobromite (Warembourg, 1993). The δ^{13}C-DIC samples for enrichment assessment were analyzed with IRMS (Thermo Scientific Delta V Advantage) coupled with Finnigan Gasbench II (Thermo Fisher Scientific). The preparation of the samples and the measurements of δ^{13}C-DIC were carried out following Torres et al. (2005).

2.5 Data analysis

Owing to the substantial effort required to measure both benthic and pelagic processes involved with N cycling, we were unable to replicate measurements spatially within a region (e.g., at multiple sites) or temporally within a season (e.g., on multiple dates). Therefore, our assessment of variation (based on replicates from single sites and dates) is likely an under-estimate of within-region and within-season variation. However, we include results from an analysis of variance as a basis for assessing the significance of differences in process rates between sites and dates. Due to a missing measurement of C-fixation at the northern site, a paired t-test was used to test for significant differences in these data. Depending on the context, both ANOVA and paired t-tests were employed to examine variations in water parameters between the two sampling dates. The assumptions of normality and homogeneity of variance were checked using the Shapiro-Wilk and Cochran's tests, respectively. In the case of heteroscedasticity, data were transformed by square $\log(1+x^2)$ or square root (sqrt). For significant factors, *post hoc* pairwise comparisons were performed using the Student-Newman-Keuls (SNK) test. The significance level was set at $\alpha = 0.05$.

Riverine NO_3^- loads to the lagoon were derived from continuous measurements of river discharge (obtained from the Lithuanian Hydrometeorological Service) and periodic measurements of riverine DIN concentrations (Figure 1). River samples were collected at approximately monthly intervals, with supplemental samples collected during periods of high discharge (March–April). Approximately 150 measurements of DIN were obtained at the river gauging station during 2012–2021. To infer daily concentrations, we modelled seasonal, inter-annual and discharge-dependent variation in riverine DIN concentrations using a Generalized Additive Model (Bukaveckas et al., 2023). The models were used to predict daily concentrations in the river, and, in combination with daily discharge, to derive daily loading values for the lagoon. Daily riverine loads were divided by the area of the lagoon to estimate the daily areal load. The average DIN load during the spring (March–May) and summer (June–August) of

2022 were used to provide a context for process measurements obtained within the lagoon on the two sampling dates.

Graphical work was performed using SigmaPlot 14.0. All data are given as mean values and standard errors based on replicates.

3 Results

3.1 Spring *vs.* summer environmental conditions

Discharge of the Nemunas River followed expected seasonal patterns, with the highest flows occurring in spring and winter (926 $m^3 s^{-1}$) and the lowest flows in summer and fall (300 $m^3 s^{-1}$, Figure 2). DIN was the dominant fraction, accounting for nearly 80% of TN in riverine inputs. NO_3^- comprised most of the DIN load and exhibited the highest concentrations in spring.

The monthly monitoring of the Curonian Lagoon showed the typical seasonal transition from N excess to limitation corresponding to variation in riverine inputs (Figure 3). The highest NO_3^- concentrations were observed in spring (April–May, mean=186.4 μmol L^{-1}, range 103.6–246.8 μmol L^{-1}) while lowest NO_3^- concentrations were in the summer (June–August, mean=0.35 μmol L^{-1}, range < 0.1–1.0 μmol L^{-1}). Nitrate concentrations in dates when benthic and pelagic processes were measured were 173.5 ± 30.4 μmol L^{-1} (May; averaged data from two sites) and 0.38 ± 0.01 μmol L^{-1} (August; averaged data from two sites). The dynamics of DSi were more intricate, with a decrease in May (0.6 ± 0.1 μmol L^{-1}) and a peak in the beginning of August (102.4 ± 16.2 μmol L^{-1}), followed by a later decrease, but still higher levels compared to the spring.

On both sampling dates when processes were measured, the water column was well-mixed, well-oxygenated (over 90% air-saturation) and of low salinity (<0.3 PSU), except for the salinity in August (1.03 PSU), when seawater entered the northern part of the lagoon (Table 2). Temperatures were lower (14.9°C *vs.* 20.5°C; t-test, t = -8,7, p ≤ 0.05) in May than in August. NO_3^- concentrations differed between the two periods (Table 3), with higher levels observed in May (SNK test, p < 0.05). In this period, NO_3^- was the dominant fraction of total nitrogen (TN), whereas in August, DON and PON accounted for the majority of TN. In May, the concentration of NO_3^- was higher at the northern (riverine) site (SNK test, p < 0.05) in comparison to the south-central (confined) site (Table 2). As water temperature increased in summer, Chl-a concentrations increased, and NO_3^- concentrations decreased in the lagoon. Similarly, the concentration of PON increased from May (range 20.5–39.9 μmol L^{-1}) to August (range 51.4–69.8 μmol L^{-1}) (Table 3) with significantly higher (SNK test, p < 0.05) concentrations at the northern site (Table 1). The changes in PON concentration were closely linked to the seasonal patterns of Chl-a (Table 2), which increased (SNK test, p < 0.05) from May to August at both sites (Table 3).

During May, the phytoplankton community mainly consisted of diatoms, which accounted for up to 77% of the total biomass (Figure 4).
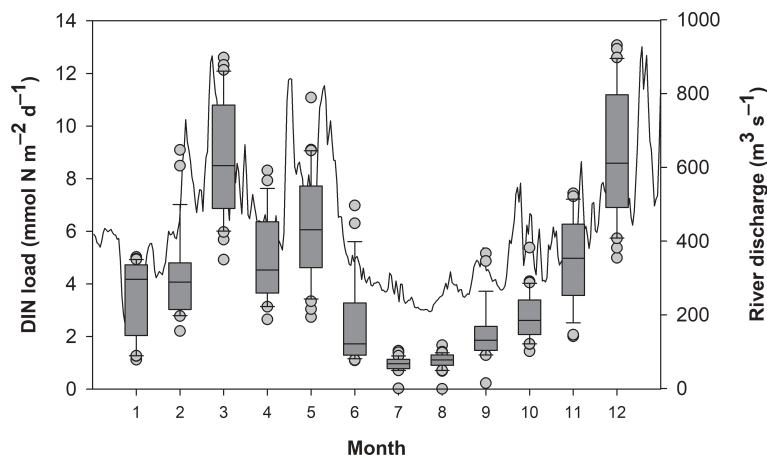
FIGURE 2
Daily discharge of the Nemunas River (black line) and monthly riverine loads of dissolved inorganic nitrogen (DIN, whisker boxes) to the Curonian Lagoon during 2021. Data range (whiskers), upper and lower quartiles (edges), the median (horizontal line), and the outliers (grey circle) are represented (n=28–31).

The dominant diatom species were *Diatoma tenuis* and *Stephanodiscus hantzschii*. In August, diatoms were replaced by cyanobacteria, which accounted for nearly 75% of total phytoplankton biomass. The dominant cyanobacteria species were non-heterocytous *Planktothrix agardhii* and heterocystous *Aphanizomenon flos-aquae*. N_2-fixing cyanobacteria (predominantly *A. flos-aquae*, *Dolichospermum affine*, and *Cuspidothrix issatschenkoi*) accounted for 14–30% of the cyanobacteria biomass. Light attenuation increased from May to August tracking changes in Chl-a. The depth of the photic zone decreased by half, causing the sediments in the shallower (northern) lagoon area to transition from photic to aphotic (Table 1). Sediments in the deeper central-southern area were aphotic during both sampling periods.

3.2 Net nitrate uptake and C-fixation in the water column

Results from tracer experiments revealed positive NO_3^- uptake rates in both light and dark bottle incubations (Figures 5A, C). Volumetric rates varied between two periods, depending on the site and irradiation regime (light *vs.* dark) (Table 3). NO_3^- uptake was higher in August than in May, with significantly higher (SNK test, ≤ 0.05) rates at the central site (0.218 ± 0.004 µmol N L^{-1} h^{-1}) compared to the northern site (0.120 ± 0.002 µmol N L^{-1} h^{-1}). At both sites, net NO_3^- uptake in the light (range 0.073–0.248 µmol N L^{-1} h^{-1}) exceeded (SNK test, ≤ 0.05) uptake in the dark (range 0.018–0.198 µmol N L^{-1} h^{-1}). When extrapolated to the entire water
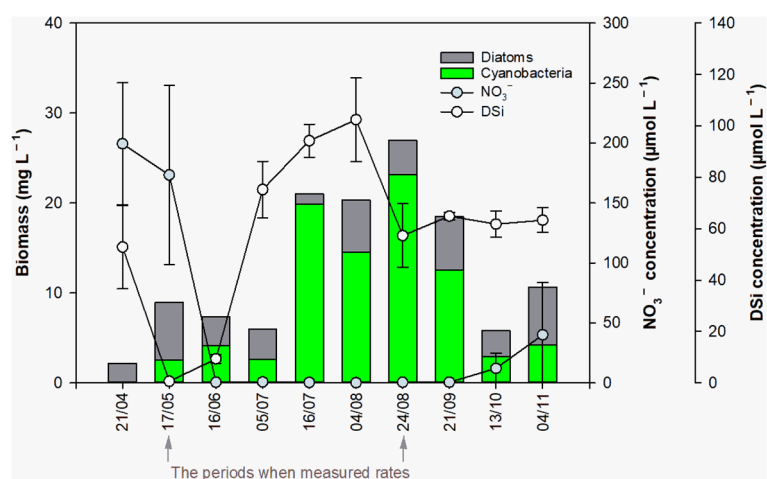
FIGURE 3
Seasonal variation in nitrate (violet circles; NO_3^-) and dissolved silica concentrations (grey circles; DSi), and diatom and cyanobacteria biomass (bars) in the Curonian Lagoon. Nutrient concentrations shown are values and standard errors (n=6) based on triplicate samples collected at stations located in the northern and south-central portions of the lagoon. Phytoplankton biomass estimates are mean values for the two sampling locations, with single samples collected from each site.

TABLE 2   Environmental conditions in the Curonian Lagoon during field campaigns to measure benthic and pelagic nitrate cycling (kd: light attenuation coefficient).

Measure	Units	May		August	
		Northern site	Central site	Northern site	Central site
kd	$[m^{-1}]$	1.42	1.21	2.02	2.39
Depth of euphotic zone	$[m]$	2	3	1.5	1.5
Temperature	$[°C]$	15.0	14.7	20.0	21.0
Salinity	$[PSU]$	0.11	0.24	1.03	0.23
NH_4^+	$[\mu mol\ L^{-1}]$	0.24 ± 0.04	0.10 ± 0.03	0.71 ± 0.12	0.12 ± 0.01
NO_3^-	$[\mu mol\ L^{-1}]$	241.6 ± 1.2	105.4 ± 0.4	0.38 ± 0.03	0.37 ± 0.02
DIN	$[\mu mol\ L^{-1}]$	243.4 ± 1.2	106.4 ± 0.4	1.15 ± 0.14	0.55 ± 0.02
DON	$[\mu mol\ L^{-1}]$	31.8 ± 2.5	15.6 ± 1.9	44.0 ± 2.0	38.8 ± 0.6
SPM	$[mg\ L^{-1}]$	10.8 ± 0.6	12.8 ± 0.8	16.1 ± 0.2	19.1 ± 3.4
PON	$[\mu mol\ L^{-1}]$	31.2 ± 10.5	39.7 ± 2.9	64.7 ± 4.7	54.0 ± 4.5
C:N in seston	$[molar]$	6.8 ± 0.1	6.6 ± 0.1	6.8 ± 0.1	6.4 ± 0.2
Chlorophyll a	$[\mu g\ L^{-1}]$	26.6 ± 0.2	29.6 ± 0.9	46.3 ± 0.7	48.8 ± 2.8

Data shown are the mean ± standard error based on three replicates.

column, results show that net daily NO_3^- uptake was lower in May (< 2 mmol N m^{-2} d^{-1}, Figures 5B, D) and higher in August, particularly at the south-central site (~15 mmol N m^{-2} d^{-1}).

The volumetric rates of C-fixation exhibited significant variations between the two periods, driven by site-specific factors (Table 3, Figures 6A, C). The highest (SNK test, p < 0.05) was found at the central site during August. C-fixation at this site was 16.1 ± 0.3 μmol C L^{-1} h^{-1}, whereas at the northern site, C-fixation was 7-fold lower (1.9 ± 0.4 μmol C L^{-1} h^{-1}; t-test, t=28.9, p < 0.001). C-fixation in the dark was low in all incubations (<0.5 μmol C L^{-1} h^{-1}). Daily- and water column-extrapolated rates varied from 26.8 to 183.3 mmol C m^{-2} d^{-1}, with the highest rates in August at the central site (Figures 6B, D). Rates of C-fixation were used to estimate phytoplankton N demand based on the C:N ratio of seston. At the central site, N demand was 4-fold higher in August (22.3 ± 0.4 mmol N m^{-2} d^{-1}) compared to May (5.6 ± 0.2 mmol N m^{-2} d^{-1}). During August, the estimated phytoplankton N demand at the northern site (3.1 ± 0.6 mmol N m^{-2} d^{-1}) was considerably lower compared to the central site (no spring data for this site).

3.3 Benthic nitrate fluxes and dissimilatory reduction processes

At both sites, rates of benthic processes were generally lower when compared to pelagic processes. Net NO_3^- fluxes at the sediment–water interface varied from –5.4 to 2.2 mmol N m^{-2} d^{-1} at the two sites. Net NO_3^- fluxes differed only between the two sampling dates (Table 3), but there was no statistically significant difference between the two sites. In May, sediments acted as a sink for NO_3^- from the overlaying water column, with a flux of –2.0 ± 0.7 mmol N m^{-2} d^{-1} (averaged data across sites), however, in August, net flux was near zero (0.01 ± 0.05 mmol N m^{-2} d^{-1}; Figures 7A, D).

Total denitrification rates (D_{tot}; 2.3 ± 0.4 mmol N m^{-2} d^{-1} averaged data) varied between two periods depending on the site (Table 3, Figures 7B, E). The site emerged as the primary factor influencing D_{tot} rates. Significantly higher D_{tot} rates (SNK test, p < 0.05) were found in the muddy sediments at the south-central site relative to the sandy sediments at the northern site. At both sites, rates were higher in May than in August (SNK test, p < 0.05). Lower denitrification rates in August were due to lower NO_3^- concentrations in the overlaying water column, as indicated by low D_w (the fraction of D_{tot} that relies on diffused NO_3^- from bottom water) in August (< 0.1 mmol N m^{-2} d^{-1}) relative to May (0.7–2.7 mmol N m^{-2} d^{-1}). Rates of coupled nitrification-denitrification (D_n) were similar during both seasons (range 0.1–1.3 mmol N m^{-2} d^{-1}), but the overall contribution to total N_2 production increased from 14% in May to 98% in August.

Rates of total DNRA exhibited significant variation across periods, contingent upon the specific site locations (Table 3, Figures 7C, F). Nevertheless, the site emerged as the most influential factor driving $DNRA_{tot}$ rates. Similarly to denitrification, DNRA in May was primarily (~80%) fueled by NO_3^- from the water column ($DNRA_w$), whereas in August, it was coupled to nitrification ($DNRA_n$). $DNRA_w$ varied between < 0.01 and 0.4 mmol N m^{-2} d^{-1}, and $DNRA_n$ varied between 0 and 0.6 mmol N m^{-2} d^{-1}, with higher rates in muddy sediments of the central site during August (0.5 ± 0.1 mmol N m^{-2} d^{-1}). At both sites, ~20% of total benthic NO_3^- reduction was attributed to $DNRA_{tot}$.

In contrast to the deeper central area, sediments in the shallower northern site were illuminated in spring, which had a significant effect on dissimilatory NO_3^- processes. During light exposure, the total denitrification rates on an hourly basis decreased by 32% compared to the rates in the dark (paired t-test, t=2.9, p ≤ 0.05). This decrease was due to the suppression of D_w and

TABLE 3 ANOVA results.

Factor	Df	SS	MS	F	p
NO_3^- concentration					
site	1	29.962	29.962	13820.9	<0.001
time	1	453.132	453.132	298768.5	<0.001
site×time	1	20.803	20.803	13716.5	<0.001
residual	8	0.012	0.0002		
total	11	494.909	44.992		
PON concentration					
site	1	3.619	3.619	0.102	0.757
time	1	1715.303	1715.303	48.461	<0.001
site×time	1	276.768	276.768	7.819	0.023
residual	8	283.164	35.396		
total	11	2278.855	207.169		
Chl-a concentration					
site	1	22.032	22.032	40.2	<0.001
time	1	1138.801	1138.801	2079.6	<0.001
site×time	1	0.235	0.235	0.4	0.531
residual	8	4.381	0.548		
total	11	1165.449	105.950		
Pelagic NO_3^- uptake					
site	1	0.021	0.021	381.9	<0.001
time	1	0.080	0.080	1463.5	<0.001
irradiation	1	0.007	0.007	131.3	<0.001
site×time	1	0.001	0.001	136.5	<0.001
site×irradiation	1	0.0003	0.0003	16.3	<0.001
time×irradiation	1	0.0004	0.0004	5.7	0.030
site×time×irradiation	1	0.0001	0.0001	7.4	0.015
residual	16	0.0001	0.0001		
total	23	0.117	0.005		
Pelagic C-fixation					
site	1	121.865	121.865	1307.6	<0.001
time	1	271.064	271.064	2908.4	<0.001
site×time	1	121.215	121.215	1300.6	<0.001
residual	8	0.746	0.093		
total	11	514.889	46.808		
Net NO_3^- fluxes					
site	1	0,018	0.018	0.2	0.692
time	1	2.888	2.888	26.1	<0.001
site×time	1	0.018	0.018	0.2	0.692
residual	16	0.177	0.110		

(Continued)

TABLE 3 Continued

Factor	Df	SS	MS	F	p
Net NO_3^- fluxes					
total	19	4.692	0.247		
Total denitrification rates (D_{tot})					
site	1	13.448	13.448	326.0	<0.001
time	1	12.800	12.800	310.3	<0.001
site×time	1	1.922	1.922	45.6	<0.001
residual	16	0.660	0.041		
total	19	28.830	1.517		
Total DNRA rates ($DNRA_{tot}$)					
site	1	0.356	0.356	45.5	<0.001
time	1	0.013	0.013	1.6	0.229
site×time	1	0.180	0.180	22.6	<0.001
residual	16	0.128	0.008		
total	19	0.686	0.036		

Df, degree of freedom; SS, sum of squares; MS, mean squares; F - F value, p - significance level, where p < 0.05.

D_n (Table 4). In contrast, DNRA was significantly (paired t-test, t=-3.1, p ≤ 0.05) stimulated by illumination, with ~90% higher rates in light incubations compared to those in the dark.

3.4 Sedimentation of particulate matter

The estimated gross sedimentation rate of suspended particulate matter (SPM) at the south-central site was 33.1 g m^{-2} d^{-1}. Assuming SPM contains 4.4% of PON (Table 2), the sedimentation of PON was calculated to be 103.7 mmol N m^{-2} d^{-1}. Considering these measured rates, nearly 53% of the PON in
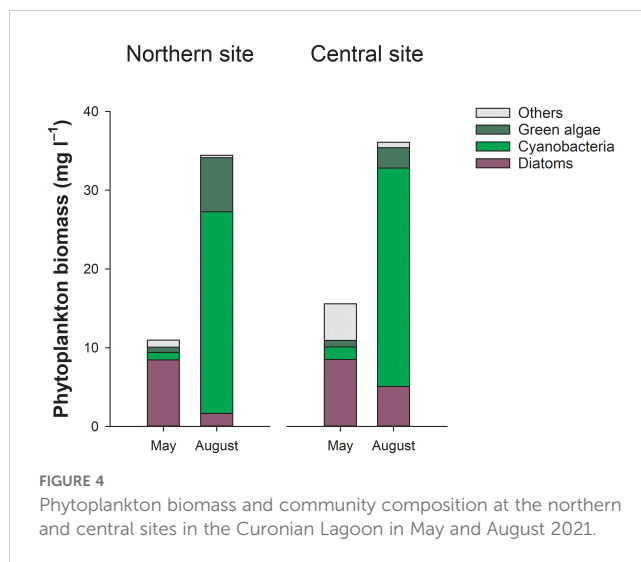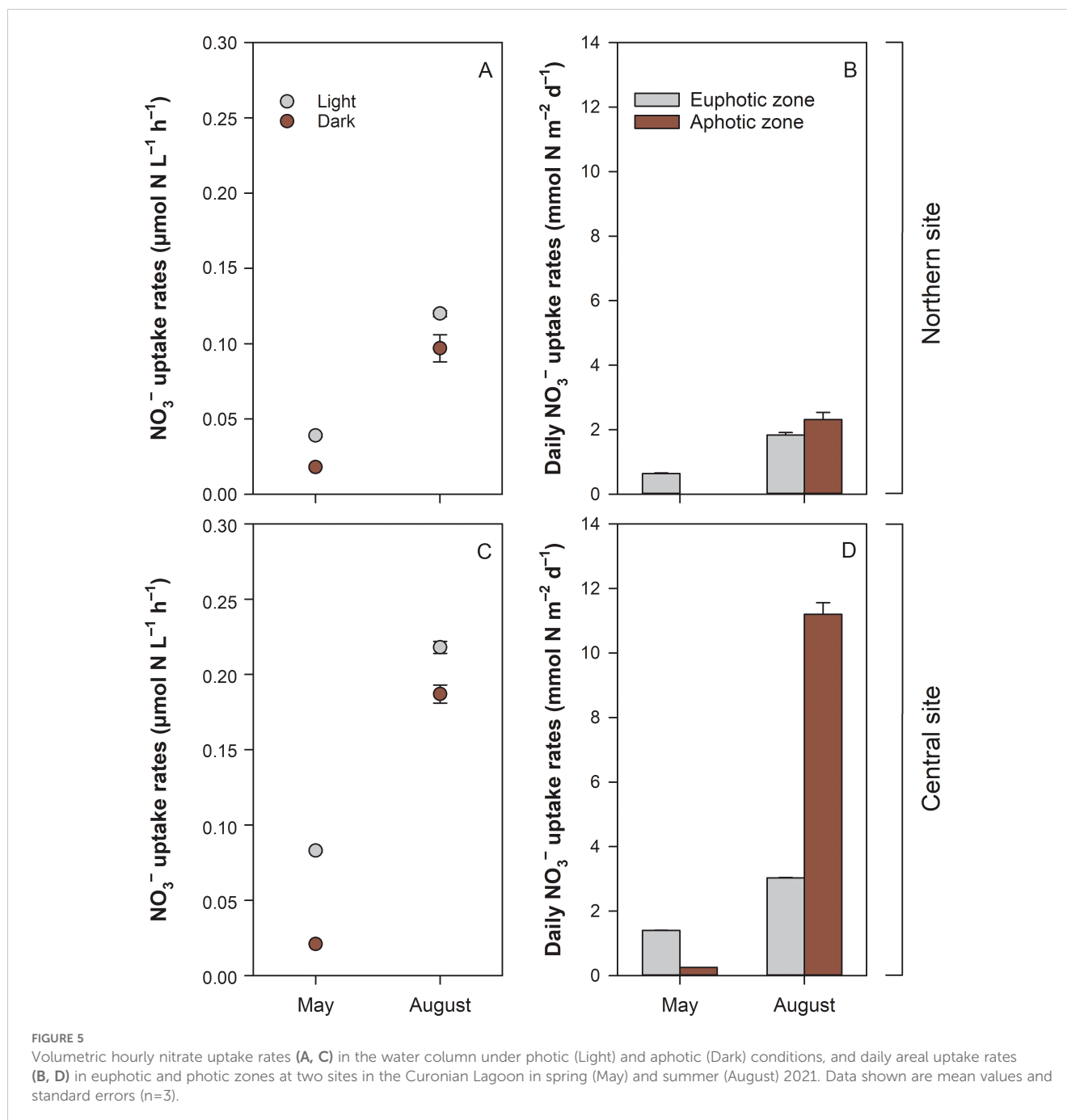

FIGURE 4
Phytoplankton biomass and community composition at the northern and central sites in the Curonian Lagoon in May and August 2021.

FIGURE 5

Volumetric hourly nitrate uptake rates **(A, C)** in the water column under photic (Light) and aphotic (Dark) conditions, and daily areal uptake rates **(B, D)** in euphotic and photic zones at two sites in the Curonian Lagoon in spring (May) and summer (August) 2021. Data shown are mean values and standard errors (n=3).

the water column (196 mmol N m^{-2} on average; Table 2) was estimated to settle to the bottom daily.

4 Discussion

4.1 Pelagic nitrate cycling pathways

A complex interaction between light and nutrient availability regulates phytoplankton growth in the Curonian Lagoon (Bartoli et al., 2021; Magri et al., 2024). The light penetration is influenced by wind-driven sediment re-suspension, while nutrient availability is regulated by seasonal variation in river nutrient inputs (Vybernaite-Lubiene et al., 2018, 2022; Zilius et al., 2014, 2018). N is commonly a limiting nutrient in coastal waters such as the Baltic Sea, and its availability typically tracks changes in NO_3^- concentrations (Vybernaite-Lubiene et al., 2017). Seasonal changes in water and NO_3^- inputs drive concurrent changes in phytoplankton abundance and community composition (Figure 2). In eutrophic waters, these are manifested as a shift from diatom-dominance in spring to cyanobacteria-dominance in summer. The influence of changes in phytoplankton communities and N availability on N cycling have not been investigated in an integrated fashion that considers the suite of relevant pelagic and benthic processes. Our data show that NO_3^- uptake rates were 65–86% higher when cyanobacteria were dominant in the summer, compared to diatom-dominated communities in the
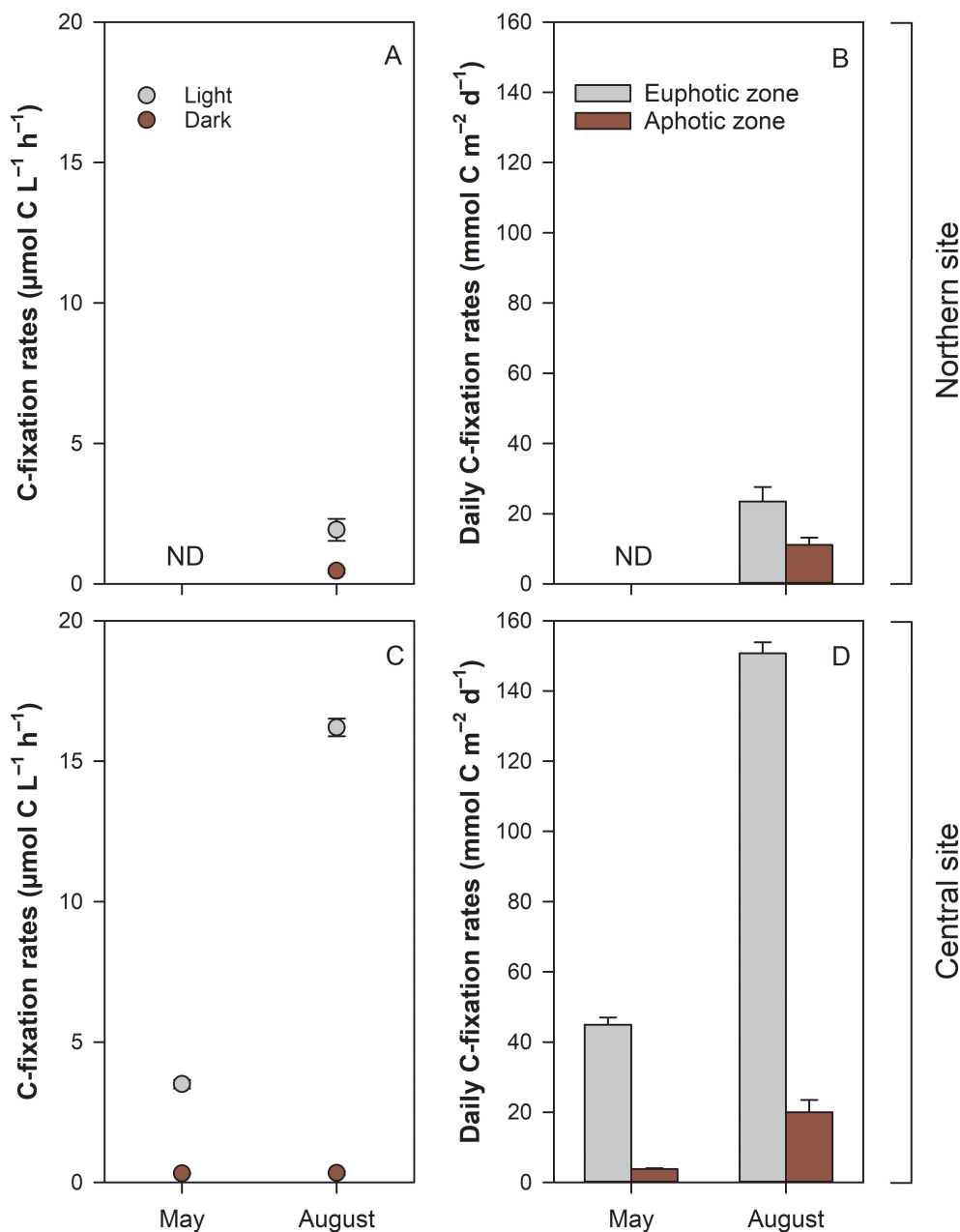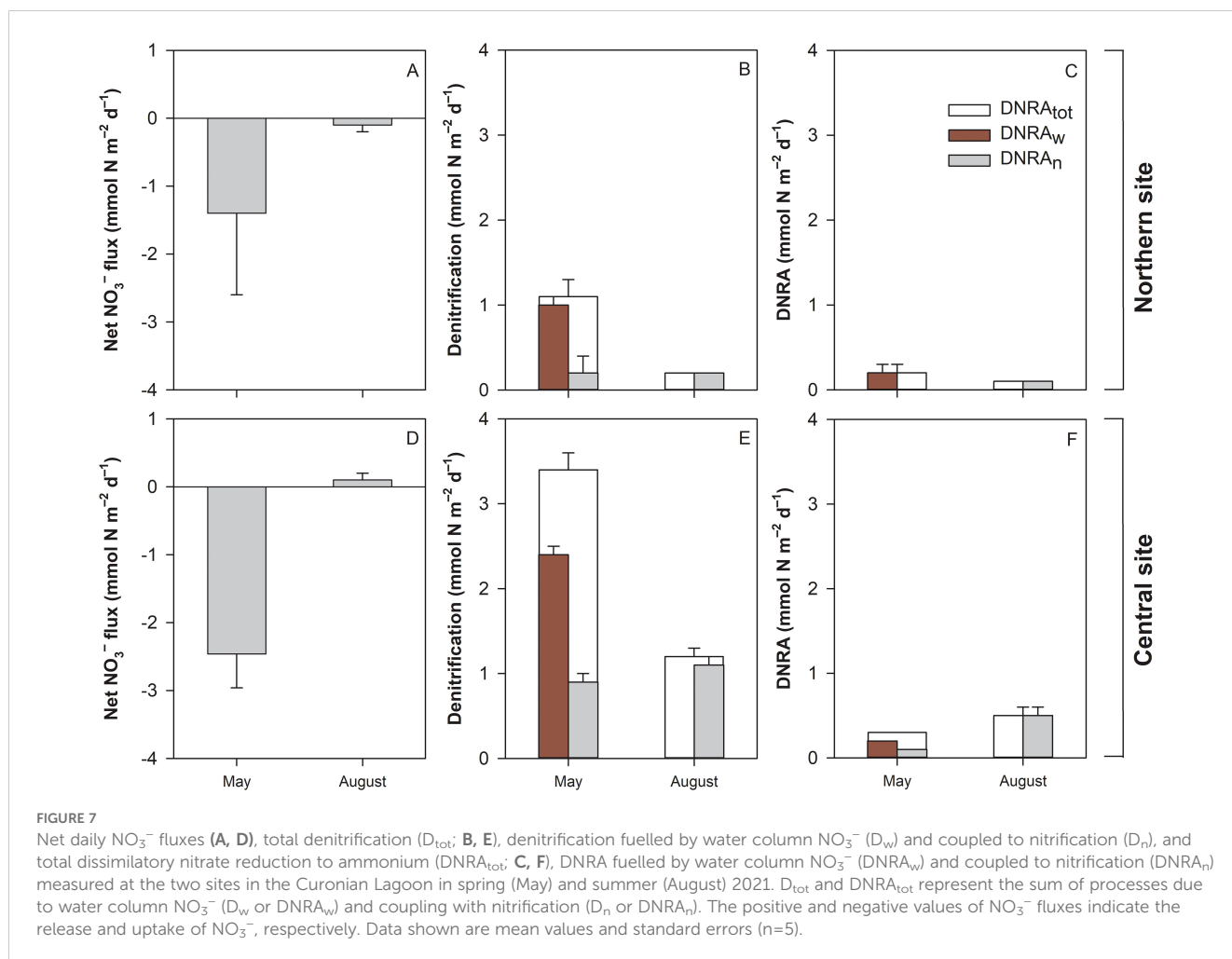
FIGURE 6
Volumetric hourly carbon fixation rates **(A, C)** in the water column under photic (Light) and aphotic (Dark) conditions, and daily areal rates **(B, D)** in euphotic and photic zones at two sites in the Curonian Lagoon in spring (May) and summer (August) 2021. Data shown are mean values and standard errors (n=3); ND — no available data.

spring. While diatoms have a higher affinity for NO_3^- (Berg et al., 2003; Lomas and Glibert, 2003; Olofsson et al., 2019), our results show that cyanobacteria-dominated communities can support higher uptake rates. This is partly attributed to the higher biomass of cyanobacteria relative to diatom biomass, but we note that mass-specific uptake rates were also higher in summer than in spring. Prior work has shown that cyanobacteria prefer NH_4^+ over NO_3^- (Chaffin and Bridgeman, 2014), but our results suggest that cyanobacteria can utilize NO_3^- efficiently, even during low DIN concentrations in summer. A comparison of NO_3^- uptake rates with estimated phytoplankton N demand (from C fixation measurements in light)

shows that the contribution of NO_3^- to the estimated phytoplankton N demand was relatively small in both spring and summer (~22% on average across sites). This suggests that NH_4^+ or DON assimilation or dinitrogen (N_2) fixation satisfied most nutritional needs for the growth of phytoplankton.

While pelagic NO_3^- uptake in spring is replenished by riverine inputs, uptake in summer would rapidly (~3 hours) deplete the small standing pool in the water column in the absence of organic matter mineralization and nitrification. In summer, the dominance of cyanobacteria may enhance N recycling in the water column (Zilius et al., 2018). Unlike fast-sinking diatoms, buoyant

FIGURE 7

Net daily NO_3^- fluxes **(A, D)**, total denitrification (D_{tot}; **B, E**), denitrification fuelled by water column NO_3^- (D_w) and coupled to nitrification (D_n), and total dissimilatory nitrate reduction to ammonium ($DNRA_{tot}$; **C, F**), DNRA fuelled by water column NO_3^- ($DNRA_w$) and coupled to nitrification ($DNRA_n$) measured at the two sites in the Curonian Lagoon in spring (May) and summer (August) 2021. D_{tot} and $DNRA_{tot}$ represent the sum of processes due to water column NO_3^- (D_w or $DNRA_w$) and coupling with nitrification (D_n or $DNRA_n$). The positive and negative values of NO_3^- fluxes indicate the release and uptake of NO_3^-, respectively. Data shown are mean values and standard errors (n=5).

cyanobacteria remain suspended in the water column (Bukaveckas et al., 2019), which may favor mineralization and nitrification in the water column over sedimentation (Peng et al., 2017; Hampel et al., 2019; Chen et al., 2021). We had previously estimated that one-third of the regenerated NH_4^+ (~30 mmol N m^{-2} d^{-1}) had the potential to undergo oxidation during nitrification (Zilius et al., 2018). In the present study, we show that nitrification in the water

column contributes ~11 mmol NO_3^- m^{-2} d^{-1}, which is comparable to net NO_3^- uptake in summer (~9.7 mmol N m^{-2} d^{-1}; Figure 8), suggesting that the NO_3^- pool turns over on a daily basis. High rates of N cycling may also be supported by utilization of DON. Our prior work has shown that much of the nitrate assimilated by phytoplankton is released as DON over short (daily) time scales (Wood and Bukaveckas, 2014). During summer, the relatively high

TABLE 4 Hourly rates (μmol N m^{-2} h^{-1}) of benthic dissimilatory nitrate (NO_3^-) reduction through denitrification and dissimilative nitrate reduction to ammonium (DNRA) under different light conditions in spring at northern (sandy) and central (muddy) sites in the Curonian Lagoon.

NO_3^- reduction process		Central site		Northern site		
		May	August	May		August
		Dark	Dark	Light	Dark	Dark
Denitrification	D_{tot}	141.0 ± 5.4	48.4 ± 2.6	24.8 ± 4.1	77.0 ± 15.3	6.7 ± 0.9
	D_w	101.9 ± 2.4	1.3 ± 0.6	22.5 ± 6.4	65.0 ± 1.0	0.1 ± 0.0
	D_n	39.1 ± 1.7	47.2 ± 2.8	2.4 ± 3.0	12.0 ± 2.9	6.6 ± 0.9
DNRA	$DNRA_{tot}$	12.7 ± 1.0	21.9 ± 1.6	14.9 ± 3.8	1.8 ± 0.1	2.3 ± 0.3
	$DNRA_w$	9.2 ± 0.8	0.6 ± 0.3	13.2 ± 3.9	1.5 ± 0.2	<0.05
	$DNRA_n$	3.5 ± 0.2	21.3 ± 1.5	1.7 ± 1.4	0.3 ± 0.0	2.3 ± 0.3

Table 1 provides details on the pathway explanations. Data shown are mean values and standard errors (n=5).
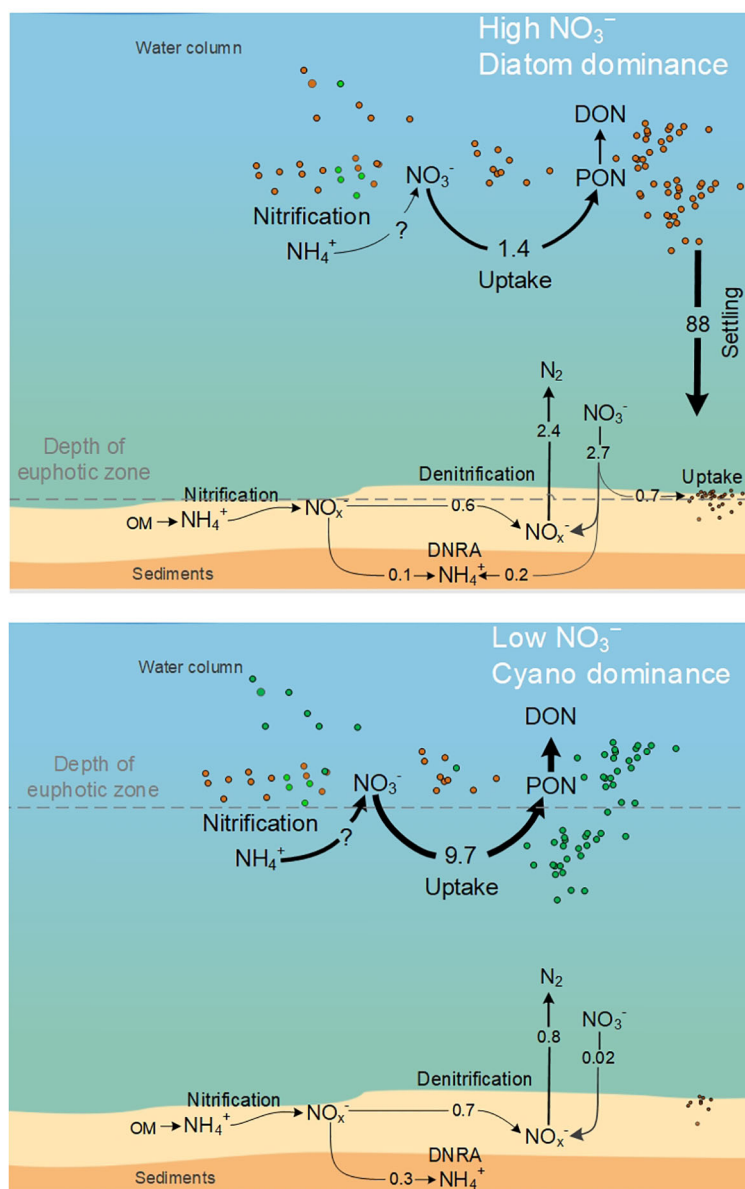
FIGURE 8
Nitrogen cycling in the Curonian Lagoon water column and sediments in spring (during diatom bloom and N excess) and summer (during cyanobacteria bloom and N scarcity). Rates are expressed as mmol N m^{-2} d^{-1}. The circle symbols indicate the relative abundance of dominant pelagic groups: diatoms (purple), cyanobacteria (light green), green algae (dark green), and others, including heterotrophs (grey).

concentration of DON compared to DIN may be important to N cycling via remineralization to NH_4^+ and oxidation to NO_3^- and via direct uptake of DON by phytoplankton (Wannicke et al., 2009; Korth et al., 2013; Zilius et al., 2018; Klawonn et al., 2019).

4.2 Benthic nitrate cycling pathways

Our findings show that rates of benthic processes differed between cyanobacteria- and diatom-dominated periods. Maximum rates of benthic NO_3^- dissimilatory processes were recorded in May during the diatom-dominated period. Our findings differ from other coastal areas of the Baltic Sea, where

sediment dissimilatory processes peaked in summer, and were attributed to the remineralization of organic matter derived from earlier inputs (Bonaglia et al., 2014; Bartl et al., 2019; Hellemann et al., 2020). Diverse seasonal patterns across coastal settings may be due to variable NO_3^- and labile organic matter availability (Hietanen and Kuoparinen, 2008; Zilius et al., 2018; Bartl et al., 2019). Higher pelagic NO_3^- concentrations associated with spring runoff and deposition of fresh organic matter following diatom blooms, are likely the primary drivers of high denitrification rates in spring. Rates measured in the Curonian Lagoon (2.3 mmol N m^{-2} d^{-1}) were appreciably higher than other coastal areas in the Baltic Sea (0.2 mmol N m^{-2} d^{-1} Gulf of Finland, Hietanen and Kuoparinen, 2008; 0.2 mmol N m^{-2} d^{-1} in Himmerfjärden

estuary, Bonaglia et al., 2014; 0.2 mmol N m^{-2} d^{-1} in Archipelago, Hellemann et al., 2020; 1.1 mmol N m^{-2} d^{-1} in Öre Estuary, Zilius et al., 2021b). By contrast, DNRA, which is rarely measured in lagoons and estuaries around the Baltic, was lower and similar among sites in the Curonian Lagoon (0.2 mmol N m^{-2} d^{-1}), the Öre Estuary (0.3 mmol N m^{-2} d^{-1}, Zilius et al., 2021b), the Himmerfjärden estuary (0.1 mmol N m^{-2} d^{-1}, Bonaglia et al., 2014) and the Gulf of Finland's archipelago (0.1 mmol N m^{-2} d^{-1}, Hellemann et al., 2020). Collectively, these findings suggest that denitrification is the main benthic process affecting water column DIN concentrations.

During summer, pelagic NO$_3^-$ concentrations were low, and the main processes responsible for the NO$_3^-$ production are mineralization and nitrification in sediments. However, ammonification rates in the sediments (up to 5 mmol N m^{-2} d^{-1}; Zilius et al., 2018) are six times lower compared to the turnover in the water column. In the south-central area of the lagoon, where organic-rich deposits accumulate, higher rates of mineralization and nitrification result in higher rates of dissimilatory NO$_3^-$ processes during the summer. Such internal NO$_3^-$ turnover via linked microbial processes is the main mechanism in other coastal settings where NO$_3^-$ is typically below <10 µmol L^{-1} throughout the year (Hellemann et al., 2020; Zilius et al., 2021b). The prevalence of denitrification over DNRA in these sediments is likely influenced by lower salinity levels (Giblin et al., 2010). Nevertheless, when brackish water intrusion leads to higher salinity, reductive processes could cause the accumulation of sulfide or reduced metal forms that may stimulate DNRA (Kessler et al., 2018; Murphy et al., 2020).

Microphytobenthos or settled phytoplankton may also play a role in the assimilation of NO$_3^-$ (Figure 8). This process is more likely to occur during spring in the shallower (northern) half of the lagoon where the benthic assimilative pathway accounts for approximately 40% of denitrification (D$_w$). Prior work by Bartoli et al. (2021) showed that deeper muddy sediments hosted only settled pelagic algae, probably because light availability strongly limited the development of a true microphytobenthos community, whereas shallower sites (<1 m) contained a mix of microphytobenthos and settled phytoplankton. In spring, there is a brief clear-water phase during which the photic zone can extend to a depth of 3 m, resulting in ~80% of the lagoon's sediment area being exposed to light. During the clear-water phase, N uptake by microalgae in shallow sandy sediments can frequently exceed the amount lost via denitrification, and photosynthetic microorganisms appear to inhibit denitrification (Sundbäck et al., 2006; Bartoli et al., 2021). Moreover, we cannot exclude the possibility that a portion of assimilated NO$_3^-$ in surface sediments is later respired through dissimilatory pathways (Merz et al., 2021).

A key result of our study is the contrasting impact of light conditions on benthic processes. Sedimentary denitrification, which was fuelled by NO$_3^-$ from the water above, was lower in the presence of light. This can be attributed to the fact that microphytobenthos are photosynthetically active. As a result, oxygen is produced and diffuses into the sediment, creating an oxic zone, which extends the diffusion pathway for NO$_3^-$ to the denitrification zone (Risgaard-Petersen, 2003). Additionally, settled

diatoms and other microphytobenthos assimilate NO$_3^-$ (Stief et al., 2022), leading to a competition between algae and heterotrophic denitrifiers (Risgaard-Petersen, 2003; Sundbäck et al., 2006). Light has also been found to enhance DNRA. The increased total DNRA rates are attributed to an increase in the uptake of ^{15}NO$_3^-$ (DNRA$_w$) from the water column. There is evidence to suggest that eukaryotic phototrophs, such as diatoms, can respire assimilated NO$_3^-$ in deeper sediment layers without oxygen and NO$_3^-$ (Merz et al., 2021). Currently, this N cycling pathway is not well understood, but it could be that settled diatoms in spring, together with prokaryotic microorganisms, may drive DNRA (Stief et al., 2022). Further work is needed to characterize the role of microphytobenthos in mediating sediment–water N fluxes and to determine whether these fluxes are influenced by changes in the abundance and composition of the benthic algal assemblage.

4.3 Algal blooms and water clarity effects on nitrate cycling

Throughout the year, the turbidity in the water column of the lagoon changes, which impacts the depth of the euphotic zone (Zilius et al., 2014). Light scattering is primarily caused by phytoplankton; in summer, cyanobacteria reduce the euphotic zone to ~1 m. As a result, the majority of the water column is in the aphotic zone, particularly in the deeper, southern part of the lagoon. During summer, when wind-driven vertical mixing is reduced, the presence of gas vesicles may allow cyanobacteria to access the narrow euphotic zone where they gain energy for NO$_3^-$ uptake and metabolism. Based on our previous metagenomics analyses, marker genes responsible for assimilative NO$_3^-$ reduction were mainly attributed to Cyanobacteria, followed by Firmicutes and Euryarcheota (Broman et al., 2021). This implies that the cyanobacterial community can assimilate NO$_3^-$ throughout the entire water column, even below the euphotic zone, and thus compete with heterotrophic microorganisms (Chaffin and Bridgeman, 2014; Hampel et al., 2019). Our results show that rates of NO$_3^-$ uptake in light were consistently higher than those in darkness (by 16–62%), indicating more effective uptake during daylight hours within the euphotic zone. In the summer, the dominant *Planktotrix* genus is adapted to lower light intensities than other cyanobacteria, making this group more competitive (Post et al., 1985). Regarding biomass, cyanobacteria dominate over other pelagic microorganisms and thus are a key component in N cycling pathways (Broman et al., 2021; Zilius et al., 2018, 2021a).

4.4 Pelagic and benthic nitrates cycling in the context of the lagoon N budget

Simultaneous measurements of pelagic and benthic NO$_3^-$ processes allowed us to develop a more complete depiction of N cycling and its contribution to NO$_3^-$ retention during spring and summer (Figure 8). During spring when diatoms dominate and NO$_3^-$ concentrations are higher, the average daily net NO$_3^-$ uptake

by sediments (2.7 mmol N m^{-2} d^{-1}) was equivalent to 41% of the daily riverine N load (mean = 6.6 mmol N m^{-2} d^{-1} in March–May). Pelagic assimilation of NO$_3^-$ (1.2 mmol N m^{-2} d^{-1}) accounted for to 18% of spring riverine N loads. Considering the high settling rates, it is likely that all assimilated NO$_3^-$ into biomass was transferred to the sediments. The combined effects of pelagic and benthic NO$_3^-$ processes could retain up to 59% of the load during spring when most of NO$_3^-$ is delivered to the system. The present study covers only two contrasting periods and sites, and additional measurement replication across seasons and sites could improve retention estimates, specifically in the spring when the two macroareas differ in water residence time, nutrient inputs and pelagic communities (Umgiesser et al., 2016; Vybernaite-Lubiene et al., 2022; Zilius et al., 2021a). We assume that in the summer, the lagoon functions more uniformly, as shown in a previous study by Zilius et al. (2021a), where upscaled pelagic rates from the two sites were representative of the whole lagoon. Expanding measurements across seasons, specifically in winter, would likely give higher denitrification rates in sediments but lower pelagic nutrient uptake rates, which may change the total NO$_3^-$ reduction rates. Overall, the estimated NO$_3^-$ retention is comparable to our previously published estimates (60% of input loads) based on an input-output mass balance (Vybernaite-Lubiene et al., 2017). The fraction of riverine inputs retained in the Curonian Lagoon exceeds other coastal settings (e.g. 12–29% in the Oder Lagoon, Grelowski et al., 2000; 18% in the Vistula Lagoon, Witek et al., 2003; 19% Archipelago Sea, Silvennoinen et al., 2007), but is similar to large embayments, such as the Stockholm Archipelago (65%, Almroth-Rosell et al., 2016). In comparison, the estuarine systems in southern Europe have relatively shorter residence times such that NO$_3^-$ inputs are rapidly flushed to adjacent coastal areas (Middelburg and Nieuwenhuize, 2000a).

In summer, pelagic demand for NO$_3^-$ increased and exceeded by 85% riverine inputs to the lagoon (1.5 mmol N m^{-2} d^{-1}). Denitrification fuelled by the water column NO$_3^-$ was negligible due to its depletion. Higher NO$_3^-$ uptake in the water column than in sediment, which was particularly notable in the south-central area, was likely due to higher cyanobacterial biomass resulting in high uptake rates (Vaičiūtė et al., 2021). NO$_3^-$ assimilation in summer is an important N cycling pathway (Broman et al., 2021), which far exceeds N inputs via biological dinitrogen fixation (2.1 mmol N m^{-2} d^{-1}; Zilius et al., 2021a) as well as NO$_3^-$ release from sediments and river inputs. This finding suggests that high rates of nitrification in the water column in the water column are needed to sustain biological NO$_3^-$ demand. Therefore, future studies should also include measurements of NO$_3^-$ production via nitrification and other cycling pathways (Figure 8).

While coupled assimilation and sedimentation temporarily retain NO$_3^-$ in the system, denitrification results in a net loss of N from the ecosystem. Comparing rates of PON deposition to the sediments with sediment denitrification (2.7 mmol N m^{-2} d^{-1}) suggests that ~6% of PON settled into the sediments is removed from the lagoon via coupled nitrification-denitrification. The majority of PON deposited to the sediments is either re-

mineralized or buried. Denitrification (D$_w$) fuelled solely by the water column NO$_3^-$ in this period was equivalent to 27% of the N load. The amount of N removed from the system is large when compared to the other coastal settings around the Baltic Sea and is highly dependent on the sediment type (e.g. 16% for the Bothnian Sea, Asmala et al., 2017). This high rate may be explained not only by high nitrate concentration but also by fresh organic matter input to the benthos (Bartoli et al., 2021). Sedimentation was not measured in summer, and it is likely low due to the dominance of buoyant cyanobacteria (Bukaveckas et al., 2019). During summer, particulate organic nitrogen was recycled in the water column to dissolved organic nitrogen, as dissolved inorganic N was relatively low or exported to the Baltic Sea with lagoon outflow (Zilius et al., 2018).

4.5 Future nitrates cycling in the lagoons

While the present study focuses on the Curonian Lagoon and its capacity to attenuate NO$_3^-$ loads, the findings can serve as a model for other Baltic lagoons. These lagoons are important ecosystems in the region, covering one-third of the Baltic coastal area (Asmala et al., 2017). Projections indicate that coastal areas of the Baltic Sea will experience changes in the future due to altered freshwater inputs, nutrient loads and rising temperatures (Meier et al., 2022; Idzelytė et al., 2023). For example, in south-eastern regions with large lagoons, nutrient loads are forecasted to increase (Hägg et al., 2014; Čerkasova et al., 2021). This is due to projected changes in snow cover, which could result in total nitrogen loads that are twice as high (Čerkasova et al., 2021). As a result, lagoons will be flushed with more NO$_3^-$, which may enhance denitrification and assimilation processes. However, changes in hydrometeorological conditions suggest the peak nutrient load will appear earlier and be shorter, meaning nutrients will be flushed to the Baltic Sea more quickly (Idzelytė et al., 2023). At the same time, the productive period in lagoons is becoming prolonged due to diminished ice cover with increasing temperatures, as indicated by earlier spring and later autumn phytoplankton blooms (Hjerne et al., 2019; Wasmund et al., 2019). Meanwhile, in summer, higher temperatures are forecasted to result in frequent heat waves (Meier et al., 2022; Safonova et al., 2024). This may enhance pelagic and benthic metabolism with increasing nutrient turnover. Given high metabolism and organic matter inputs from the water column, bottom water and sediments can become anoxic (e.g. Zilius et al., 2014). While this may facilitate the water column and sediment denitrification process, it will become negligible if no NO$_3^-$ exists in lagoons. The future direction of lagoon shifts remains uncertain as these estuarine systems and overall shallow coastal areas in the Baltic region have received limited attention. As a result, baseline information that could indicate tipping points is lacking. Consequently, common efforts to examine Baltic lagoons will provide this critical data and allow for more accurate prediction of trajectories in nutrient biogeochemistry over time.

5 Conclusions

This study provides insights into how variable riverine inputs and phytoplankton seasonal succession affect rates of pelagic and benthic N cycling in a shallow coastal lagoon. In spring, benthic processes were important as diatom blooms and elevated riverine inputs favored high rates of denitrification and net flux of N from the water column to the sediments. In summer, cyanobacteria-dominated blooms caused high rates of pelagic assimilation, which, coupled with low riverine inputs, resulted in the depletion of DIN and minimal N fluxes across the sediment–water interface. Denitrification dominated in spring, while DNRA remained low in both seasons, pointing to the important control of labile organic matter deposition from settling phytoplankton. Our findings are consistent with the paradigm that eutrophication favors a shift from benthic to pelagic-dominated processes. Furthermore, these findings suggest that the greater prevalence of cyanobacteria, while enhancing pelagic DIN recycling within the lagoon, results in greater export of DON and PON relative to periods dominated by diatom communities.

Data availability statement

The raw data supporting the conclusions of this article will be made available by the authors, without undue reservation.

Author contributions

MZ: Writing – original draft, Conceptualization, Funding acquisition, Investigation, Methodology. RB: Data curation, Formal analysis, Investigation, Writing – review & editing. SB: Data curation, Formal analysis, Funding acquisition, Methodology, Writing – review & editing. IK: Conceptualization, Methodology, Writing – review & editing. EL: Data curation, Formal analysis, Investigation, Writing – review & editing. TP: Data curation, Formal analysis, Investigation, Writing – review & editing. IV-L: Data curation, Formal analysis, Investigation, Writing – review & editing. MV: Data curation, Resources, Writing – review & editing. DO: Data curation, Investigation, Writing – review & editing. PB: Writing – original draft, Writing – review & editing.

Conflict of interest

The authors declare that the research was conducted in the absence of any commercial or financial relationships that could be construed as a potential conflict of interest.

Publisher's note

All claims expressed in this article are solely those of the authors and do not necessarily represent those of their affiliated organizations, or those of the publisher, the editors and the reviewers. Any product that may be evaluated in this article, or claim that may be made by its manufacturer, is not guaranteed or endorsed by the publisher.

Supplementary material

The Supplementary Material for this article can be found online at: https://www.frontiersin.org/articles/10.3389/fmars.2024.1497246/full#supplementary-material

References

Almroth-Rosell, E., Edman, M., Eilola, K., Meier, M. H. E., and Sahlberg, J. (2016). Modelling nutrient retention in the coastal zone of an eutrophic sea. *Biogeosciences* 13, 5753–5769. doi: 10.5194/bg-13-5753-2016

Anderson, I. C., Brush, M. J., Piehler, M. F., Currin, C. A., Stanhope, J. W., Smyth, A. R., et al. (2014). Impacts of climate-related drivers on the benthic nutrient filter in a shallow photic estuary. *Estuaries Coast.* 37, 46–62. doi: 10.1007/s12237-013-9665-5

Arheimer, B., Dahne, J., and Donnelly, C. (2012). Climate change impact on riverine nutrient load and land-based remedial measures of the Baltic Sea Action Plan. *Ambio* 41, 600–612. doi: 10.1007/s13280-012-0323-0

Asmala, E., Carstensen, J., Conley, D. J., Slomp, C. P., Stadmark, J., and Voss, M. (2017). Efficiency of the coastal filter: Nitrogen and phosphorus removal in the Baltic Sea. *Limnol. Oceanogr.* 62, S222–S238. doi: 10.1002/lno.10644

Bartl, I., Hellemann, D., Rabouille, C., Schulz, K., Tallberg, P., Hietanen, S., et al. (2019). Particulate organic matter controls benthic microbial N retention and N removal in contrasting estuaries of the Baltic Sea. *Biogeosciences* 16, 3543–3564. doi: 10.5194/bg-16-3543-2019

Bartoli, M., Nizzoli, D., Zilius, M., Bresciani, M., Pusceddu, A., Bianchelli, S., et al. (2021). Denitrification, nitrogen uptake, and organic matter quality undergo different seasonality in sandy and muddy sediments of a turbid estuary. *Front. Microbiol.* 11. doi: 10.3389/fmicb.2020.612700

Berg, G. M., Balode, M., Purina, I., Bekere, S., Béchemin, C., and Maestrini, S. Y. (2003). Plankton community composition in relation to availability and uptake of oxidized and reduced nitrogen. *Aquat. Microbiol. Ecol.* 30, 263–274. doi: 10.3354/ame030263

Bonaglia, S., Deutsch, B., Bartoli, M., Marchant, H. K., and Brüchert, V. (2014). Seasonal oxygen, nitrogen and phosphorus benthic cycling along an impacted Baltic Sea estuary: regulation and spatial patterns. *Biogeochemistry* 119, 139–160. doi: 10.1007/s10533-014-9953-6

Brion, N., Andersson, M. G. I., Elskens, M., Diaconu, C., Baeyens, W., Dehairs, F., et al. (2008). Nitrogen cycling, retention and export in a eutrophic temperate macrotidal estuary. *Mar. Ecol. Progr. Ser.* 357, 87–99. doi: 10.3354/meps07249

Broman, E., Zilius, M., Samuiloviene, A., Vybernaite-Lubiene, I., Politi, T., Klawonn, I., et al. (2021). Active DNRA and denitrification in oxic hypereutrophic waters. *Water Res.* 194), 116954. doi: 10.1016/j.watres.2021.116954

Bukaveckas, P. A., Barisevičiūtė, R., Zilius, M., Vybernaite-Lubiene, I., Petkuviene, J., Vaiciute, D., et al. (2023). Carbon fluxes from River to sea: sources and fate of carbon in a shallow, coastal lagoon. *Estuaries Coast.* 46, 1223–1238. doi: 10.1007/s12237-023-01214-w

Bukaveckas, P. A., Barry, L. E., Beckwith, M. J., David, V., and Lederer, B. (2011). Factors determining the location of the chlorophyll maximum and the fate of algal production within the tidal freshwater James River. *Estuaries Coast.* 34, 569–582. doi: 10.1007/s12237-010-9372-4

Bukaveckas, P. A., Beck, M., Devore, D., and Lee, W. M. (2018). Climatic variability and its role in regulating C, N and P retention in the James River Estuary. *Estuar. Coast. Shelf Sci.* 205, 161–173. doi: 10.1016/j.ecss.2017.10.004

Bukaveckas, P. A., Katarzyte, M., Schlegel, A., Spuriene, R., Egerton, T., and Vaiciute, D. (2019). Composition and settling properties of suspended particulate matter in estuaries of the Chesapeake Bay and Baltic Sea regions. *J. Soils Sediment.* 19, 2580–2593. doi: 10.1007/s11368-018-02224-z

Carstensen, J., Conley, D. J., Almroth-Rosell, E., Asmala, E., Bonsdorff, E., Fleming-Lehtinen, V., et al. (2020). Factors regulating the coastal nutrient filter in the Baltic Sea. *Ambio* 49, 1194–1210. doi: 10.1007/s13280-019-01282-y

Čerkasova, N., Umgiesser, G., and Ertürk, A. (2021). Modelling framework for flow, sediments and nutrient loads in a large transboundary river watershed: A climate change impact assessment of the Nemunas River watershed. *J. Hydrol.* 598, 126422. doi: 10.1016/j.jhydrol.2021.126422

Chaffin, J. D., and Bridgeman, T. B. (2014). Organic and inorganic nitrogen utilization by nitrogen-stressed cyanobacteria during bloom conditions. *J. Appl. Phycol.* 26, 299–309. doi: 10.1007/s10811-013-0118-0

Chen, X., Wang, K., Li, X., Qiao, Y., Dong, K., and Yang, L. (2021). Microcystis blooms aggravate the diurnal alternation of nitrification and nitrate reduction in the water column in Lake Taihu. *Sci. Total Environ.* 767, 144884. doi: 10.1016/j.scitotenv.2020.144884

Dong, L. F., Smith, C. J., Papaspyrou, S., Stott, A., Osborn, A. M., and Nedwell, D. B. (2009). Changes in benthic denitrification, nitrate ammonification, and anammox process rates and nitrate and nitrite reductase gene abundances along an estuarine nutrient gradient (the Colne Estuary, United Kingdom). *Appl. Environ. Microb.* 75 (10). doi: 10.1128/AEM.02511-08

Dong, L. F., Thornton, D. C. O., Nedwell, D. B., and Underwood, G. J. C. (2000). Denitrification in sediments of the River Colne estuary, England. *Mar. Ecol. Progr. Ser.* 203, 109–122. doi: 10.3354/meps203109

Dortch, Q. (1990). The interaction between ammonium and nitrate uptake in phytoplankton. *Mari. Ecol. Progr. Ser.* 61, 183–201. doi: 10.3354/meps061183

Dugdale, R. C., and Wilkerson, F. P. (1986). The use of ^{15}N to measure nitrogen uptake in eutrophic oceans; experimental considerations. *Limnol. Oceanogr.* 31, 673–689. doi: 10.4319/lo.1986.31.4.0673

Giblin, A. E., Weston, N. B., Banta, G. T., Tucker, J., and Hopkinson, C. S. (2010). The effects of salinity on nitrogen losses from an oligohaline estuarine sediment. *Estuaries Coast.* 33, 1054–1068. doi: 10.1007/s12237-010-9280-7

Glibert, P. M., Wilkerson, F. P., Dugdale, R. C., Raven, J. A., Dupont, C., Leavitt, P. R., et al. (2016). Pluses and minuses of ammonium and nitrate uptake and assimilation by phytoplankton and implications for productivity and community composition, with emphasis on nitrogen-enriched conditions. *Limnol. Oceanogr.* 61, 165–197. doi: 10.1002/lno.10203

Grasshoff, K., Ehrhardt, M., and Kremling, K. (1983). *Methods of seawater analysis. 2nd edn* (Berlin: Verlag Berlin Chemie).

Grelowski, A., Pastuszak, M., Sitek, S., and Witek, Z. (2000). Budget calculations of nitrogen, phosphorus and BOD$_5$ passing through the Oder estuary. *J. Mar. Syst.* 25, 221–237. doi: 10.1016/S0924-7963(00)00017-8

Hägg, H. E., Lyon, S. W., Wällstedt, T., Mörth, C.-M., Claremar, B., and Humborg, C. (2014). Future nutrient load scenarios for the baltic sea due to climate and lifestyle changes. *Ambio* 43, 337–351. doi: 10.1007/s13280-013-0416-4

Hampel, J., McCarthy, M. J., Neudeck, M., Bullerjahn, G. S., McKay, R. M. L., and Newell, S. E. (2019). Ammonium recycling supports toxic *Planktothrix* blooms in Sandusky Bay, Lake Erie: Evidence from stable isotope and metatranscriptome data. *Harmful Algae* 81, 42–52. doi: 10.1016/j.hal.2018.11.011

HELCOM (2021). *Guidelines for monitoring of phytoplankton species composition, abundance and biomass* (Helsinki, Finland: HELCOM), 22pp. doi: 10.25607/OBP-1822

Hellemann, D., Tallberg, P., Aalto, S. L., Bartoli, M., and Hietanen, S. (2020). Seasonal cycle of benthic denitrification and DNRA in the aphotic coastal zone, northern Baltic Sea. *Mar. Ecol. Progr. Ser.* 637, 15–28. doi: 10.3354/meps13259

Hietanen, S., and Kuoparinen, J. (2008). Seasonal and short-term variation in denitrification and anammox at a coastal station on the Gulf of Finland, Baltic Sea. *Hydrobiologia* 596, 67–77. doi: 10.1007/s10750-007-9058-5

Hjerne, O., Hajdu, S., Larsson, U., Downing, A. S., and Winder, M. (2019). Climate driven changes in timing, composition and magnitude of the Baltic Sea phytoplankton spring bloom. *Front. Mar. Sci.* 6. doi: 10.3389/fmars.2019.00482

Idzelytė, R., Čerkasova, N., Dabulevičienė, T., Razinkovas-Baziukas, A., Ertürk, A., and Umgiesser, G. (2023). Coupled hydrological and hydrodynamic modelling application for climate change impact assessment in the Nemunas River watershed–Curonian Lagoon–south-eastern Baltic Sea continuum. *Ocean Sci.* 19, 1047–1066. doi: 10.5194/os-19-1047-2023

Jakimavičius, D., and Kriaučiūnienė, J. (2013). The climate change impact on the water balance of the Curonian Lagoon. *Water Resour* 40, 120–132. doi: 10.1134/S0097807813020097

Jeffrey, S. T., and Humphrey, G. F. (1975). New spectrophotometric equations for determining chlorophylls a, b, c1 and c2 in higher plants, algae and natural phytoplankton. *Biochem. Physiol. Pflanz (BPP)* 167, 191–194. doi: 10.1016/S0015-3796(17)30778-3

Kessler, A., Roberts, K. R., Bissett, A., and Cook, P. L. M. (2018). Biogeochemical controls on the relative importance of denitrification and dissimilatory nitrate reduction to ammonium in estuaries. *Glob. Biogeochem. Cycles* 32, 1045–1057. doi: 10.1029/2018GB005908C

Killberg-Thoreson, L., Baer, S. E., Sipler, R. E., Reay, W. G., Roberts, Q. N., and Bronk, D. A. (2021). Seasonal nitrogen uptake dynamics and harmful algal Blooms in the York River, Virginia. *Estuaries Coast.* 44, 750–768. doi: 10.1007/s12237-020-00802-4

Klawonn, I., Bonaglia, S., Whitehouse, M. J., Littmann, S., Tienken, D., Kuypers, M. M. M., et al. (2019). Untangling hidden nutrient dynamics: rapid ammonium cycling and single-cell ammonium assimilation in marine plankton communities. *ISME J.* 13, 1960–1974. doi: 10.1038/s41396-019-0386-z

Korth, F., Fry, B., Liskow, I., and Voss, M. (2013). Nitrogen turnover during the spring outflows of the nitrate-rich Curonian and Szczecin lagoons using dual nitrate isotopes. *Mar. Chem.* 154, 1–11. doi: 10.1016/j.marchem.2013.04.012

Lomas, M. W., and Glibert, P. M. (2003). Comparisons of nitrate uptake, storage, and reduction in marine diatoms and flagellates. *J. Phycol.* 36, 903–913. doi: 10.1046/j.1529-8817.2000.99029.x

Magri, M., Benelli, S., Bonaglia, S., Zilius, M., Castaldelli, G., and Bartoli, M. (2020). The effects of hydrological extremes on denitrification, dissimilatory nitrate reduction to ammonium (DNRA) and mineralization in a coastal lagoon. *Sci. Total Environ.* 740, 140169. doi: 10.1016/j.scitotenv.2020.140169

Magri, M., Bondavalli, C., Bartoli, M., Benelli, S., Zilius, M., Petkuviene, J., et al. (2024). Temporal and spatial differences in nitrogen and phosphorus biogeochemistry and ecosystem functioning of a hypertrophic lagoon (Curonian Lagoon, SE Baltic Sea) revealed via Ecological Network Analysis. *Sci. Total Environ.* 921, 171070. doi: 10.1016/j.scitotenv.2024.171070

Meier, H. E. M., Dieterich, C., Gröger, M., Dutheil, C., Börgel, F., Safonova, K., et al. (2022). Oceanographic regional climate projections for the Baltic Sea until 2100. *Earth Syst. Dynam.* 13, 159–199. doi: 10.5194/esd-13-159-2022

Merz, E., Dick, G. J., de Beer, D., Grim, S., Hübener, T., Littmann, S., et al. (2021). Nitrate respiration and diel migration patterns of diatoms are linked in sediments underneath a microbial mat. *Environ. Microb.* 23, 1422–1435. doi: 10.1111/1462-2920.15345

Middelburg, J. J., and Nieuwenhuize, J. (2000a). Uptake of dissolved inorganic nitrogen in turbid, tidal estuaries. *Mar. Ecol. Progr. Ser.* 192, 79–88. doi: 10.3354/meps192079

Middelburg, J. J., and Nieuwenhuize, J. (2000b). Nitrogen uptake by heterotrophic bacteria and phytoplankton in the nitrate-rich Thames estuary. *Mar. Ecol. Progr. Ser.* 203, 13–21. doi: 10.3354/meps203013

Montoya, P. J., Voss, M., Kähler, P., and Capone, D. G. (1996). A simple, high-precision, high-sensitivity tracer assay for N$_2$ fixation. *Appl. Environ. Microbiol.* 62, 986–993. doi: 10.1128/aem.62.3.986-993.1996

Murphy, A. E., Bulseco, A. N., Ackerman, R., Vineis, J. H., and Bowen, J. L. (2020). Sulphide addition favours respiratory ammonification (DNRA) over complete denitrification and alters the active microbial community in salt marsh sediments. *Environ. Microb.* 22, 2124–2139. doi: 10.1111/1462-2920.14969

Nielsen, L. P. (1992). Denitrification in sediment determined from nitrogen isotope pairing. *FEMS Microbiol. Lett.* 86, 357–362. doi: 10.1111/j.1574-6968.1992.tb04828.x

Olenina, I., Hajdu, S., Edler, L., Andersson, A., Wasmund, N., Busch, S., et al. (2006). "Biovolumes and size-classes of phytoplankton in the Baltic Sea," in *HELCOM Baltic Sea environmental proceedings*, Vol. 106. 144.

Olofsson, M., Robertson, E. K., Edler, L., Arneborg, L., Whitehouse, M. J., Ploug, H., et al. (2019). Nitrate and ammonium fluxes to diatoms and dinoflagellates at a single cell level in mixed field communities in the sea. *Sci. Rep.* 9, 1424. doi: 10.1038/s41598-018-38059-4

Parson, T. R., Maita, Y., and Lalli, C. M. (1984). *A manual of chemical and biological methods for seawater analysis* (New York: Pergamon Press).

Peierls, B., Caraco, N., Pace, M., and Cole, J.J. (1991). Human influence on river nitrogen. *Nature* 350, 386–387. doi: 10.1038/350386b0

Peng, Y., Liu, L., Jiang, L., and Xiao, L. (2017). The roles of cyanobacterial bloom in nitrogen removal. *Sci. Total Environ.* 609, 297–303. doi: 10.1016/j.scitotenv.2017.03.149

Politi, T., Zilius, M., Forni, P., Zaiko, A., Daunys, D., and Bartoli, M. (2022). Biogeochemical buffers in a eutrophic coastal lagoon along an oxic-hypoxic transition. *Estuar. Coast. Shelf Sci.* 279, 108132. doi: 10.1016/j.ecss.2022.108132

Post, A. F., Loogman, J. G., and Mur, L. R. (1985). Regulation of growth and photosynthesis by *Oscillatoria agardhii* grown with a light/dark cycle. *FEMS Microbiol. Ecol.* 1, 97–102. doi: 10.1111/j.1574-6968.1985.tb01136.x

Risgaard-Petersen, N. (2003). Coupled nitrification-denitrification in autotrophic and heterotrophic estuarine sediments: on the influence of benthic microalgae. *Limnol. Oceanogr.* 48, 93–105. doi: 10.4319/lo.2003.48.1.0093

Safonova, K., Meier, H. E. M., and Gröger, M. (2024). Summer heatwaves on the Baltic Sea seabed contribute to oxygen deficiency in shallow areas. *Commun. Earth. Environ.* 5, 106. doi: 10.1038/s43247-024-01268-z

Santos, I. R., Chen, X., Lecher, A. L., Sawyer, A. H., Moosdorf, N., Rodellas, V., et al. (2021). Submarine groundwater discharge impacts on coastal nutrient biogeochemistry. *Nat. Rev. Earth Environ.* 2, 307–323. doi: 10.1038/s43017-021-00152-0

Silvennoinen, H., Hietanen, S., Liikanen, A., Stange, C. F., Russow, R., Kuparinen, J., et al. (2007). Denitrification in the river estuaries of the northern Baltic Sea. *Ambio* 36, 134–140. doi: 10.1579/0044-7447(2007)36[134:DITREO]2.0.CO;2

Stief, P., Schauberger, C., Lund, M. B., Greve, A., Abed, R. M. M., Al-Najjar, M. A. A., et al. (2022). Intracellular nitrate storage by diatoms can be an important nitrogen pool in freshwater and marine ecosystems. *Commun. Earth Environ.* 3, 154. doi: 10.1038/s43247-022-00485-8

Sundbäck, K., Miles, A., and Linares, F. (2006). Nitrogen dynamics in nontidal littoral sediments: Role of microphytobenthos and denitrification. *Estuaries Coast.* 29, 1196–1211. doi: 10.1007/BF02781820

Thamdrup, B. (2012). New pathways and processes in the global nitrogen cycle. *Ann. Rev. Ecol. Evol. S.* 43, 407–428. doi: 10.1146/annurev-ecolsys-102710-145048

Torres, M. E., Mix, A. C., and Rugh, W. D. (2005). Precise δ^{13}C analysis of dissolved inorganic carbon in natural waters using automated headspace sampling and continuous-flow mass spectrometry. *Limnol. Oceanogr.-M.* 3, 349–360. doi: 10.4319/lom.2005.3.349

Twomey, L. J., Piehler, M. F., and Paerl, H. W. (2005). Phytoplankton uptake of ammonium, nitrate and urea in the Neuse River Estuary, NC, USA. *Hydrobiologia* 533, 123–134. doi: 10.1007/s10750-004-2403-z

Umgiesser, G., Zemlys, P., Erturk, A., Razinkova-Baziukas, A., Mėžinė, J., and Ferrarin, C. (2016). Seasonal renewal time variability in the Curonian Lagoon caused by atmospheric and hydrographical forcing. *Ocean Sci.* 12, 391–402. doi: 10.5194/os-12-391-2016

Utermöhl, H. (1958). Zur Vervollkommnung der quantitativen Phytoplankton-Methodik. *Int. Assoc. Theor. Appl. Limnol.* 9, 1–38.

Vaičiūtė, D., Bučas, M., Bresciani, M., Dabulevičienė, T., Gintauskas, J., Mėžinė, J., et al. (2021). Hot moments and hotspots of cyanobacteria hyperblooms in the Curonian Lagoon (SE Baltic Sea) revealed via remote sensing-based retrospective analysis. *Sci. Total Environ.* 769, 145053. doi: 10.1016/j.scitotenv.2021.145053

Veuger, B., Middelburg, J. J., Boschker, H. T. S., Nieuwenhuize, J., van Rijswijk, P., Rochelle-Newall, E. J., et al. (2004). Microbial uptake of dissolved organic and inorganic nitrogen in Randers Fjord. *Estuar. Coast. Shelf Sci.* 61, 507–515. doi: 10.1016/j.ecss.2004.06.014

Voss, M., Baker, A., Bange, H. W., Conley, D., Cornell, S., Deutsch, B., et al. (2011). *Nitrogen processes in coastal and marine ecosystems* (Cambridge: Cambridge University Press), 147–176.

Voss, M., Deutsch, B., Liskow, I., Pastuszak, M., Schulte, U., and Sitek, S. (2010). Nitrogen retention in the Szczecin lagoon, Baltic Sea. *Isot. Environ. Health Stud.* 46, 355–369. doi: 10.1080/10256016.2010.503895

Vybernaite-Lubiene, I., Zilius, M., Bartoli, M., Petkuviene, J., Zemlys, P., Magri, M., et al. (2022). Biogeochemical budgets of nutrients and metabolism in the Curonian Lagoon (South East Baltic Sea): Spatial and temporal variations. *Water* 14, 164. doi: 10.3390/w14020164

Vybernaite-Lubiene, I., Zilius, M., Giordani, G., Petkuviene, J., Vaiciute, D., Bukaveckas, P. A., et al. (2017). Effect of algal blooms on retention of N, Si and P in Europe's largest coastal lagoon. *Estuar. Coast. Shelf Sci.* 194, 217–228. doi: 10.1016/j.ecss.2017.06.020

Vybernaite-Lubiene, I., Zilius, M., Saltyte-Vaisiauske, L., and Bartoli, M. (2018). Recent Trends, (2012–2016) of N, Si, and P export from the Nemunas River watershed: loads, unbalanced stoichiometry, and threats for downstream aquatic ecosystems. *Water* 10, 1178. doi: 10.3390/w10091178

Wannicke, N., Koch, B. P., and Voss, M. (2009). Release of fixed N_2 and C as dissolved compounds by *Trichodesmium* erythreum and Nodularia spumigena under the influence of high light and high nutrient (P). *Aquat. Microb. Ecol.* 57, 175–189. doi: 10.3354/ame01343

Wasmund, N., Nausch, G., Gerth, M., Busch, S., Burmeister., C., Hansen, R., et al. (2019). Extension of the growing season of phytoplankton in the western Baltic Sea in response to climate change. *Mar. Ecol. Prog. Ser.* 622, 1–16. doi: 10.3354/meps12994

Warembourg, F. R. (1993). "Nitrogen fixation in soil and plant systems," in *Nitrogen isotope techniques*, vol. 127–156 . Eds. R. Knowles and T. H. Blackburn (Academic Press, San Diego).

Witek, Z., Humborg, C., Savchuk, O., Grelowski, A., and Lysiak-Pastuszak, E. (2003). Nitrogen and phosphorus budgets of the Gulf of Gdansk (Baltic Sea). *Estuar. Coast. Shelf Sci.* 57, 239–248. doi: 10.1016/S0272-7714(02)00348-7

Wood, J. D., and Bukaveckas, P. A. (2014). Increasing severity of phytoplankton nutrient limitation following reductions in point source inputs to the tidal freshwater segment of the James River Estuary. *Estuaries Coast.* 37, 1188–1201. doi: 10.1007/s12237-013-9756-3

Zemlys, P., Ferrarin, C., Umgiesser, G., Gulbinskas, S., and Bellafiore, D. (2013). Investigation of saline water intrusions into the Curonian Lagoon (Lithuania) and two-layer flow in the Klaipèda Strait using finite element hydrodynamic model. *Ocean Sci.* 9, 573–584. doi: 10.5194/os-9-573-2013

Zilius, M. (2011). Oxygen and nutrient exchange at the sediment-water interface in the eutrophic boreal lagoon (Baltic Sea). University of Klaipeda, Lithuania.

Zilius, M., Bartoli, M., Bresciani, M., Katarzyte, M., Ruginis, T., Petkuviene, J., et al. (2014). Feedback mechanisms between cyanobacterial blooms, transient hypoxia, and benthic phosphorus regeneration in shallow coastal environments. *Estuaries Coast.* 37, 680–694. doi: 10.1007/s12237-013-9717-x

Zilius, M., Bartoli, M., Daunys, D., Pilkaityte, R., and Razinkovas, A. (2012). Patterns of benthic oxygen uptake in a hypertrophic lagoon: spatial variability and controlling factors. *Hydrobiologia* 699, 85–98. doi: 10.1007/s10750-012-1155-4

Zilius, M., Daunys, D., Bartoli, M., Marzocchi, U., Bonaglia, S., Cardini, U., et al. (2021b). Partitioning benthic nitrogen cycle processes among three common macrofauna holobionts. *Biogeochemistry* 157, 193–213. doi: 10.1007/s10533-021-00867-8

Zilius, M., Samuiloviene, A., Stanislauskienė, A., Broman, E., Bonaglia, S., Meškys, R., et al. (2020). Depicting temporal, functional, and phylogenetic patterns in estuarine diazotrophic communities from environmental DNA and RNA. *Microb. Ecol.* 81, 36–51. doi: 10.1007/s00248-020-01562-1

Zilius, M., Vybernaite-Lubiene, I., Vaiciute, D., Overlingė, D., Grinienė, E., Zaiko, A., et al. (2021a). Spatiotemporal patterns of N_2 fixation in coastal waters derived from rate measurements and remote sensing. *Biogeosciences* 18, 1857–1871. doi: 10.5194/bg-18-1857-2021

Zilius, M., Vybernaite-Lubiene, I., Vaiciute, D., Petkuviene, J., Zemlys, P., Liskow, I., et al. (2018). The influence of cyanobacteria blooms on the attenuation of nitrogen throughputs in a Baltic coastal lagoon. *Biogeochemistry* 141, 143–165. doi: 10.1007/s10533-018-0508-0